MEIOSIS INITIATES IN THE FETAL OVARY OF MICE LACKING ALL RETINOIC ACID RECEPTOR ISOTYPES

Nadège VERNET[1], Manuel MARK[1,2], Diana CONDREA[1], Betty FÉRET[1], Muriel KLOPFENSTEIN[1], Violaine ALUNNI[3], Marius TELETIN[1,2], and Norbert B. GHYSELINCK[1*]

1. Institut de Génétique et de Biologie Moléculaire et Cellulaire (IGBMC), Département de Génétique Fonctionnelle et Cancer, Centre National de la Recherche Scientifique (CNRS UMR7104), Institut National de la Santé et de la Recherche Médicale (INSERM U1258), Université de Strasbourg (UNISTRA), 1 rue Laurent Fries, BP-10142, F-67404 Illkirch Cedex, France
2. Service de Biologie de la Reproduction, Hôpitaux Universitaires de Strasbourg (HUS), France
3. GenomEast platform, France Génomique consortium, IGBMC, 1 rue Laurent Fries, F-67404 Illkirch Cedex, France

* Author for correspondence: norbert@igbmc.fr

Tel: +33 388 655 674; Fax: +33 388 653 201

Abstract

Gametes are generated through a specialized cell differentiation process, meiosis which, in most mammals, is initiated in ovaries during fetal life. It is widely admitted that all-*trans* retinoic acid (ATRA) is the molecular signal triggering meiosis initiation in mouse female germ cells, but a genetic approach in which ATRA synthesis is impaired disputes this proposal. In the present study, we investigated the contribution of endogenous ATRA to meiosis by analyzing fetuses lacking all RARs ubiquitously, obtained through a tamoxifen-inducible cre recombinase-mediated gene targeting approach. Efficient ablation of RAR-coding genes was assessed by the multiple congenital abnormalities displayed by the mutant fetuses. Unexpectedly, their germ cells robustly expressed STRA8, REC8, SYCP1 and SYCP3, showing that RAR are actually dispensable up to the zygotene stage of meiotic prophase I. Thus our study goes against the current model according to which meiosis is triggered by endogenous ATRA in the developing ovary and revives the identification of the meiosis-preventing substance synthesized by CYP26B1 in the fetal testis.

Introduction

Mammalian meiosis is a germ-cell specific division process that generates haploid gametes from their diploid precursors, oogonia in the female and spermatogonia in the male. In the mouse, female germ cells enter into meiosis before birth, around embryonic day 13.5 (E13.5)[1]. During the same embryonic period, male germ cells stop proliferating, and enter the G0/G1 phase of the cell cycle thus becoming mitotically quiescent. Male germ cells resume proliferation at birth, and then enter into meiosis starting from post-natal day 8[2].

In order to account for the sexual dimorphism in the timing of gem cell differentiation, it was hypothesized, notably from transplantation experiments of germ cells[3], that the decision to enter meiosis is controlled by a meiosis-inducing substance (MIS) or/and by a meiosis-preventing substance (MPS) produced by somatic cells[4]. Subsequently, it was proposed that all-trans retinoic acid (ATRA) and its degrading enzyme CYP26B1 played key roles in controlling the timing of meiosis initiation in female and male gonads, respectively[5,6]. The concept that ATRA is the MIS was however challenged by a genetic study demonstrating that meiosis initiation occurs despite the lack of two major ATRA-synthesizing enzymes[7]. The recent finding that a third enzyme, expressed in fetal ovaries and capable of ATRA synthesis, is also involved in meiosis revived the model according to which meiosis entry is triggered by endogenous ATRA in the ovary[8]

ATRA is the active metabolite of retinol (vitamin A). Inside cells, conversion of retinol to ATRA depends upon retinaldehyde dehydrogenases (ALDH1A1, ALDH1A2 and ALDH1A3 isotypes)[9]. Then, ATRA activity is mediated by the nuclear retinoic acid receptors (RARA, RARB and RARG isotypes), which are ligand-dependent transcriptional regulators. They usually function in the form of heterodimers with

rexinoid receptors (RXRs) to control expression of ATRA-target genes, in which they are bound to specific DNA sites called retinoic acid response elements (RARE)[10]. In addition, RAR are capable of non-genomic activation events at the cell membrane[11], similarly to steroid nuclear receptors[12].

As all ATRA-dependent events rely in some way on RAR, we decided to tackle the potential contribution of endogenous ATRA to meiosis in female germ cells by generating and analyzing mice lacking all RAR-isotypes. Against the currently admitted model[13,14], our study reveals that RARs (and therefore endogenous ATRA) are in fact fully dispensable for meiotic initiation in the mouse fetal ovary.

Results

Expression of RARs in the fetal ovary

The expression of *Rars* in the fetal gonads is poorly documented[15-17]. To determine which RAR isotypes are actually present in the ovary, we performed immunohistochemistry (IHC). At E11.5, RARA was detected in a large number of tissues, including the somatic cells of the ovary but not germ cells (**Fig. 1A,C-E**). No information was obtained for RARB since reliable antibodies for RARB are not available[18]. RARG was readily detected in cartilages, but not in the ovary (**Fig. 1B-B'**). Then we performed RT-qPCR on single ovarian cells at E13.5 (n=25) and E14.5 (n=40), to which the germ cell identity was assigned based on the expression of *Dazl*, *Ddx4* and *Kit*. *Rara* and *Rarg* mRNAs were detected in a majority of germ cells at E13.5 and E14.5 (**Fig. 1F,G**). No information was obtained for *Rarb* mRNA since the mice we used were on a *Rarb*-null genetic background (see Methods). It is therefore evident that at least two RAR mRNAs are present in female germ cells, but at some stage their level of expression is below the threshold of detection by IHC.

Efficient ablation of all RARs in the developing gonad from E11.5 onwards

Given the expression pattern of RARs, we reasoned that full impairment of ATRA signaling in the whole fetal ovary would require the ablation of all three RAR-coding genes. This was not possible by associating *Rara*, *Rarb* and *Rarg* knockout alleles in a single fetus, because $Rara^{-/-}$;$Rarg^{-/-}$;$Rarb^{+/-}$ embryos do not develop beyond E8.5, precluding analysis of their ovaries[19]. To do so, we performed cre-directed genetic ablation of *Rara* and *Rarg* using a ubiquitously expressed cre/ERT^2 activated by TAM, prior to meiotic initiation, but later than E8.5, in the context of a *Rarb*-null background (see Methods). We first chose to administer TAM at E10.5, shortly after the start of

gonad formation, but three days before meiosis initiation. Ablation of RARA and RARG was assessed by IHC at E11.5, i.e., 24 hours after TAM-induction of cre/ERT^2. Immunostaining for RARG was nearly abolished in mutant embryos in all RARG-expressing tissues. Only a few cells reacted with the antibody (**Suppl. Fig. 1**). At E14.5, the number of cells remaining positive for RARG in mutants was even smaller, while no cell expressed RARA (**Suppl. Fig. 2**). Thus efficient ablation of RARA and RARG was widespread at E11.5 and complete at E14.5.

The pattern of gene excision by cre/ERT^2 was assessed using the *mT/mG* reporter transgene in control and mutant fetuses (see Methods). Expression of mGFP was detected in all germ cells of the mutants at E11.5, and in almost all of them at E14.5 (**Suppl. Fig. 3**). This indicated that cre/ERT^2-directed excision of the reporter occurred in almost all germ cells, as early as 24 hours after TAM treatment. In agreement with this finding, *Rara* and *Rarg* mRNAs were not detected in any germ cell isolated from mutant ovaries at E13.5 or E14.5, and analyzed by RT-qPCR (**Fig. 1G**). Altogether, these data showed that efficient excision of all RARs occurred in all germ cells.

Ablation of all RARs does not impair meiosis initiation

To investigate the impact of RAR ablation on meiotic initiation, the expression of canonical markers of meiosis was assessed by IHC throughout the anteroposterior axis of the ovary. At E14.5, numerous germ cells in both control and mutant fetuses expressed the synaptonemal protein SYCP3[20] and the cohesin REC8[21] (**Fig. 2A**). The mean number of germ cells, and the percentages of SYCP3-positive or REC8-positive germ cells were similar in control and mutant fetuses (**Fig. 2B,C**). This indicated that meiosis initiated in germ cells of the mutant fetuses.

To rule out the possibility that the cells which initiated meiosis experienced an inefficient ablation of the RAR-coding genes, we took advantage of the presence of *mT/mG* reporter in the fetuses. The vast majority of the SYCP3- or REC8-positive germ cells of the mutant ovary were mGFP-positive (**Fig. 3A-F**), indicating excision in almost all of the meiotic cells. Surprisingly, mGFP was never detected in somatic cells of the ovary nor in the mesonephros, making questionable whether cre/ERT^2 was efficient or whether the reporter was expressed in these cells. To assess RAR ablation in somatic cells and exclude the possibility that cre-mediated excision was mosaic, we performed genomic PCR analysis, using DNA extracted from whole ovaries of E13.5 control and mutant fetuses. Excised (L-), but not conditional (L2), alleles of *Rara* and *Rarg* were detected in genomic DNA isolated from mutant ovaries. In contrast, conditional (L2), but not excised (L-), alleles were always detected in control ovaries (**Fig. 3G,H**). Altogether, these data show that efficient excision of all RARs occurs in all of their tissues, including somatic and germ cells in the ovaries.

To further investigate expression of the meiotic program at the cellular level in the absence of RARs, we used RT-qPCR on single cells isolated from ovaries at E13.5 (25 control and 43 mutant germ cells) and E14.5 (40 control and 47 mutant germ cells). Consistent with IHC analyses, the proportion of germ cells expressing *Sycp3* and *Rec8*, as well as their individual levels of expression, were similar in control and mutant ovaries (**Fig. 3I**). In addition, the cellular expression of 12 other meiosis-specific genes including some of the ATRA-dependent class 1 to 3 genes[22] (*Dmc1*, *Mei1*, *Meiob*, *Prdm9*, *Smc1b*, *Spo11*, *Stag3*, *Syce1*, *Syce2*, *Sycp1*, *Sycp2*, *Ugt8a*) was similar, whether RAR were present or absent (**Suppl. Figs. 4-6**). This confirmed the commitment of mutant germ cells toward meiosis, despite their lack of RARs.

Importantly, the meiotic gatekeeper STRA8[23] was also expressed in germ cells of mutant ovaries, notably in those which underwent cre/ERT^2-mediated recombination (**Fig. 3C,F**), albeit their number was about half-less that observed in control ovaries (**Fig. 2C**). Accordingly, *Stra8* mRNA was present in only 30% of the germ cells from mutant ovaries at E13.5, versus 92% in control ovaries. In addition, its expression level was slightly decreased, when compared to the control situation (**Fig. 3I**). This difference was smoothed out at E14.5 in mutant germ cells where the expression level of *Stra8* almost reached that measured in control germ cells at E13.5 (**Fig. 3I**). These observation suggested that *Stra8* expression might be delayed in the absence of RARs.

Ablation of RARs at an earlier developmental stage dramatically impacts embryonic development but not meiosis initiation

When treated by TAM at 10.5, the mutant fetuses displayed, at E14.5, some of the eye defects typically observed in *Rarb*$^{-/-}$;*Rarg*$^{-/-}$ knockout fetuses (**Suppl. Fig. 7**). However, overall these mutant fetus were much less malformed than expected from previous works[24]. For instance, the cardiac defects described in *Rara*$^{-/-}$;*Rarg*$^{-/-}$ knockout fetuses[25] were not observed. To test for the possibility that this discrepancy could be due to the timing of RARs ablation, we treated pregnant females with TAM at E9.5, and analyzed the phenotypes induced in fetuses at E14.5. The mutants generated in this way displayed most of the congenital malformations that are hallmarks of the loss of RARs[24] (**Fig. 4**). We conclude therefore that deletion of RARs with TAM at E9.5 recapitulates the pathological phenotypes observed in the compound knockouts of RARs (i.e., in *Rara*$^{-/-}$;*Rarb*$^{-/-}$, *Rara*$^{-/-}$;*Rarg*$^{-/-}$ and *Rarb*$^{-/-}$;*Rarg*$^{-/-}$ fetuses).

Given the role assigned to ATRA in sex determination[26] and primordial germ cells proliferation[27,28], one might have expected that deleting RARs at E9.5 would affect the

gonads more dramatically than at E10.5. Yet, ovaries formed in mutants and contained normal amounts of germ cells, out of which many of them were meiotic, as indicated by their expression of SYCP3 at E14.5 (**Suppl. Fig. 8**).

To test for the possibility of a delay in meiosis entry in the absence of RAR (see above), we analyzed at E15.5 control and mutant ovaries of fetuses treated by TAM at E9.5. Virtually all germ cells had entered meiosis in the mutant ovaries, as attested by the detection of SYCP3 in almost all germ cells (**Fig. 5A,B**). Moreover, a majority of the germ cells showed thread-like segments of synaptonemal complexes positive for only SYCP3 or SYCP1 and SYCP3, indicating that they were at the late leptotene to zygotene stages (**Fig. 5C,D**). Both REC8 and STRA8 were detected at E15.5 in a few germ cells from control and mutant ovaries (**Fig. 5E-H**), as expected from previous studies[29,30]. Altogether, our results indicate that RARs are indispensable neither to enter meiosis, nor to express STRA8 in germ cells. Importantly, no increase of apoptosis was evidenced in the mutant ovaries, excluding thereby the possibility that some of the RAR-deficient germ cells experienced cell-death. We conclude that in females, RARs are not required for gonad differentiation nor for meiosis, up to the zygotene stage.

Discussion

It is widely believed that ATRA synthesized by the mesonephros is an essential paracrine factor diffusing into the ovary to trigger the differentiation of oogonia to oocytes, which progress into meiosis[13,31-36]. Nonetheless, germ cells can initiate meiosis in the absence of ALDH1A2, the ATRA-synthesizing enzyme detected in the mesonephros[7]. This seemingly contradictory data has been the source of heated and passionate debates[14,37] but the discovery that the weak ATRA-synthesizing enzyme ALDH1A1 is capable of generating some ATRA in the developing mouse ovary[8,38] tailored an explanation for the finding that ovarian germ cells remain able to enter meiosis in *Aldh1a2*$^{-/-}$ knockout fetuses[8,35]. We designed the present genetic study, in which ATRA-receptors are deleted, to address by another mean the question as to whether or not ATRA is required to meiosis initiation in the mouse female germ cells.

Our results clearly show that meiotic cells expressing STRA8, REC8 and SYCP3 are present in ovaries lacking RARs. Both the number of STRA8-positive cells and the level of *Stra8* expression are lower in mutant than in control ovaries at E13.5. However, this difference diminishes at E14.5, and at E15.5 the proportion of oocytes that are at the late leptotene and zygotene stages is similar in mutant and control ovaries. It is therefore reasonable to propose that RARs participate to the timed expression of *Stra8* in the fetal ovary but, are actually not indispensable. Actually, other transcription factors such as MSX1, MSX2[39] and DMRT1[40], other signaling pathways such as BMPs[39,41] and Activin A[42], as well as the epigenetic status of chromatin[43,44] appear more important than ATRA for proper *Stra8* expression in the fetal ovary.

More intriguingly, single cell RT-qPCR analyses at E13.5 reveal that some control and most RAR-null oocytes express meiotic genes such as *Dmc1*, *Smc1b*, *Spo11*, *Stag3*, *Syce1*, *Syce2*, before expressing *Stra8*. Nonetheless, meiosis progresses up

to the zygotene stage at E15.5, despite the delay in *Stra8* expression. This finding suggests that *Stra8* expression is not be the primary event triggering meiosis in oocytes, which is unexpected given its assigned central role in this process[23]. Accordingly, *Stra8*-deficient ovarian germ cells can grow and differentiate into oocyte-like cells, without premeiotic chromosomal replication, synapsis and recombination[45]. Analysis of RAR-deficient oocytes beyond zygotene would certainly be informative, but is unfortunately not possible because RAR-null mutant fetuses die at birth from multiple congenital abnormalities[24].

The finding that RARs are crucial for neither *Stra8* expression nor meiosis initiation implies that ATRA is not the molecule triggering meiosis, provided it does not act through a RAR-independent mechanism. Several reports describe binding of ATRA to nuclear receptors other than RARs. First, peroxisome proliferator activated receptor delta (PPARD) is activated by ATRA when the latter is delivered bound to FABP5. The interaction of ATRA with PPARD has a Kd of 15–50 nM[46], more than two order of magnitude weaker than that of RAR, which is in the 0.1–0.2 nM range[47,48]. This concentration of ATRA is much higher than that observed in the fetal mouse ovary[7] or required for *Stra8* expression[36]. In addition, *Fabp5* is not expressed in the mouse fetal ovary[16], and *Ppard*-null females are fertile, indicating normal meiosis[49,50]. Second, the chicken ovalbumin upstream promoter transcription factor (NR2F2) and the testicular receptor 4 (NR2C2) can be activated by ATRA, but at non-physiological concentrations of 10-30 µM[51,52]. Third, ATRA binds to the retinoic acid receptor-related orphan receptor beta (RORB) with a Kd of 0.3 µM, but *Rorb*-null females are fertile[53]. Aside from nuclear receptors, cellular retinoic acid binding protein 1 (CRABP1) is also able to mediate some non-genomic activity of ATRA at a concentration of 100 nM[54]. However, CRABP1-null mice are fertile, and their ovaries appears fully normal[55-57].

Since all the mechanisms identified to date through which ATRA could act independently of RARs can be excluded, ATRA is not the meiosis inducing substance. In agreement with this view, the report by Chassot et al. (accompanying manuscript) shows that simultaneous ablation of *Aldh1a1*, *Aldh1a2* and *Aldh1a3* in either the somatic cells or in the whole ovary of mice do not impair *Stra8* expression and meiosis initiation. These findings are in keeping with the recent observation that initiation of meiosis and expression of *Stra8* by spermatocytes occurs without ATRA[58].

Our results apparently contradict previous observations[13,31-36], but several explanations can be proposed to reconcile the discrepancies. First, experiments performed using BMS-204493[6,29,41] and AGN193109[5,8,26,38] to impair ATRA signaling in fetal ovaries or testes must be interpreted with caution. Actually these ligands are not RAR antagonists, as they are usually referred to as, but pan-RAR inverse agonists, which are capable of repressing RAR basal activity by favoring and stabilizing recruitment of corepressors, even in the absence of an endogenous agonistic ligand such as ATRA[59-62]. As RAR binding sites are present in the *Stra8* promoter on which RARs are actually bound *in vivo*[7,63,64], adding a pan-RAR inverse agonist predictably induces recruitment of NCOR1 and NCOR2 corepressors at the locus, promotes chromatin compaction[65] and thereby *Stra8* extinction, irrespective of the presence of ATRA in the ovary. The same holds true for the *Rec8* gene, which also contains a RARE[63,66]. The fact that expression of these two genes is artificially shut down upon exposure to a pan-RAR inverse agonist does not mean that their expression is normally controlled by endogenous ATRA. If one assumes that *Rec8* and *Stra8* are actually not regulated by endogenous ATRA, it is perfectly logical to find them expressed in germ cells lacking RARs (present study). For the same reason, the fact that AGN193109 abrogates the ectopic expression of *Stra8* in *Cyp26b1*-null mouse testes is not a proof

that expression of *Stra8* depends on ATRA signaling. Therefore it cannot be used as an argument to quash the theory proposed by Kumar et al. in 2011 that a molecule distinct from ATRA is involved in the initiation of meiosis[8]. Second, it has been recurrently emphasized that alterations generated by exogenously administered ATRA do not necessarily reflect physiological processes[24,67-69]. In the case of the gonads, the simple fact that RAR-binding sites are present in *Stra8* and *Rec8* genes can explain their forced expression and initiation of meiosis by supra-physiological concentrations of ATRA added to fetal rat ovaries[70] and to mouse testes cultured *in vitro*[5,6].

Involvement of ATRA in meiosis is commonly interpreted according to the prevailing idea according which both a MIS, ATRA, and a MPS, the ATRA-degrading enzyme CYP26B1, are required to account for the sex-specific timing of meiotic initiation[13,14]. Since the present work disqualifies ATRA as an MIS, the “MPS-only” hypothesis[71] would reconcile the discrepancies present in the literature: germ cells are programmed to initiate meiosis unless prevented from doing so by an MPS produced in the testis[72]. According to this scenario, inducing mitotic quiescence instead of meiosis in male germ cells during fetal life requires a yet unknown substance, the MPS, which is undoubtedly produced by CYP26B1[7,73]. Efforts should now be put to identify this substance.

Methods

Mice and treatments

Mice were on a mixed C57BL/6 (50%)/129/SvPass (50%) genetic background. They were housed in a licensed animal facility (agreement #C6721837). All experiments were approved by the local ethical committee (Com'Eth, accreditations APAFIS#5638-2016061019045714 and APAFIS#5639-201606101910981), and were supervised by N.B.G., M.M. and N.V., who are qualified in compliance with the European Community guidelines for laboratory animal care and use (2010/63/UE). To inactivate *Rar* coding genes, mice bearing *lox*P-flanked (L2) alleles of *Rara*[74] and *Rarg*[75] and null (L-) alleles of *Rarb*[76,77] were crossed with mice bearing the ubiquitously expressed, tamoxifen-inducible, cre/ERT^2 recombinase-coding *Tg*(*Ubc-cre/ERT^2* transgene[78]. Females homozygous for L2 alleles of *Rara* and *Rarg* and for L- alleles of *Rarb* (i.e., *Rara*$^{L2/L2}$;*Rarg*$^{L2/L2}$;*Rarb*$^{L-/L-}$) were mated with males bearing one copy of the *Tg*(*Ubc-cre/ERT^2*), and homozygous for L2 alleles of *Rara* and *Rarg* and for L- alleles of *Rarb* (i.e., *Tg*(*Ubc-cre/ERT^2*);*Rara*$^{L2/L2}$;*Rarg*$^{L2/L2}$;*Rarb*$^{L-/L-}$). Noon of the day of a vaginal plug was taken as 0.5 day embryonic development (E0.5). To activate the cre/ERT2 recombinase in embryos, one tamoxifen (TAM) treatment (130 mg/kg body weight) was administered to the pregnant females by oral gavage at E9.5 or at E10.5. TAM (T5648, Sigma-Aldrich) was dissolved in ethanol at a concentration of 100 mg/mL and further diluted in sunflower oil to a concentration of 10 mg/ml. This resulted in embryos or fetuses null for *Rarb* in which *Rara* and *Rarg* were ablated upon TAM induction when they were bearing *Tg*(*Ubc-cre/ERT^2*) (referred to as mutants), as well as their control littermates when the embryos or fetuses were free of *Tg*(*Ubc-cre/ERT^2*) (referred to as controls). Importantly, embryos, fetuses and females null for *Rarb* display normal ovaries and are totally fertile[76,77]. To assess for cre/ERT^2-directed excision, we

297 introduced the *Gt(ROSA26)*$^{ACTB\text{-}tdTomato\text{-}EGFP}$ reporter transgene (referred to as *mT/mG*),
298 which directs expression of a membrane-targeted green fluorescent protein (mGFP) in
299 cells that have experienced cre-mediated deletion[79], in the *Tg*(*Ubc-*
300 *cre/ERT2*);*Rara*$^{L2/L2}$;*Rarg*$^{L2/L2}$;*Rarb*$^{L-/L-}$ genetic background. Embryos and fetuses were
301 collected by caesarean section and the yolk sacs, tail biopsies or female gonads were
302 taken for DNA extraction. Genotypes were determined as described[74-76,78,79].

303 **External morphology, histology and immunohistochemistry**

304 Following collection, E11.5 embryos to E15.5 fetuses were fixed overnight in cold 4%
305 (w/v) paraformaldehyde (PFA) in phosphate buffered saline (PBS). After removal of
306 the fixative, embryos and fetuses were rapidly rinsed in PBS and placed in 70% (v/v)
307 ethanol for long-term storage and external morphology evaluation. They were next
308 embedded in paraffin. Consecutive, frontal, 5 µm-thick sections were made throughout
309 the entire specimens. For histology, sections were stained with hematoxylin and eosin
310 (H&E). For immunohistochemistry (IHC) antigen were retrieved for 1 hour at 95°C
311 either in 10 mM sodium citrate buffer at pH 6.0 or, only in the case of IHC for detection
312 of REC8 and SYCP1, in Tris-EDTA at pH 9.0 [10 mM Tris Base, 1 mM EDTA, 0.05%
313 (v/v) Tween 20]. Sections were rinsed in PBS, then incubated with appropriate dilutions
314 of the primary antibodies or a mixture of them (i.e., anti-DDX4 and anti-SYCP3; anti-
315 SYCP1 and anti-SYCP3) in PBS containing 0.1% (v/v) Tween 20 (PBST) for 16 h at
316 4°C in a humidified chamber. After rinsing in PBST (3 times for 3 min each), detection
317 of the bound primary antibodies was achieved for 45 min at 20°C in a humidified
318 chamber using Cy3-conjugated donkey anti-rabbit, Alexa Fluor 488-conjugated
319 donkey anti-mouse or goat anti-chicken antibodies, depending on the origin of the
320 primary antibody depending on the origin of the primary antibody (**Suppl. Table 1**).

Nuclei were counterstained with 4',6-diamidino-2-phenyl-indole (DAPI) diluted at 10 µg/ml in the mounting medium (Vectashield; Vector).

Characterization and counts of the meiotic germ cells

Germ cell counts were performed on pairs of fetuses consisting of one mutant and one of its control littermates, and each experiment was repeated on at least 3 different fetuses per genotype, age and stage of TAM treatment. The total number of germ cells in ovaries of control and mutant E14.5 fetuses was quantified using immunostaining for DDX4. Meiotic germ cells were quantified using immunostaining for SYCP3, REC8 and STRA8. A double-immunostaining for SYCP1 and SYCP3 was performed to detect germ cells at the zygotene stage. Data were expressed as percentages related to the number of DDX4-positive cells. Statistical analysis was done by a two-tail Student *t*-test, assuming unequal variances after arcsine transformation of the percentages of germ cells expressing the meiotic markers.

Single cell RT-qPCR and data processing

Gonads from E13.5 and E14.5 control and mutant fetuses were dissected out in PBS and sexed by their appearance under the microscope. Ovaries were separated from mesonephros using the cutting edge of a 25G needle. Dissociated cells were obtained by incubating the gonads for 15 minutes in PBS containing 0.5 µM EDTA[80]. To allow cell pricking, gonads were then transferred in PBS containing 4 mg/ml BSA. Cells were released by puncture of the gonad with 25G needles. This technique generally resulted in a suspension of germ cells, which are recognized as large, refringent, cells, with low somatic cell contamination[81]. Cells (n=88 at E13.5 and n=132 at E14.5), were collected individually using pulled Pasteur pipets, and transferred as isolated, single, cells into micro-tubes containing 5 µl of cold 1X SuperScript IV VILO Master Mix for two-step RT-qPCR containing 6 units RNasin (Promega) and 0.5% (v/v) NP40. The micro-tubes

were then stored at -80°C for later processing. Two-step, single-cell, gene expression analysis was achieved on the BioMark HD system (Fluidigm) using SsoFast EvaGreen Supermix with low ROX (Bio-Rad Laboratories) according to manufacturer's instructions. The set of primers used for qPCR are listed (**Suppl. Table 2**). Cts were recovered and analyzed by the Fluidigm Real-Time PCR Analysis software, using the linear (derivative) baseline correction method and the auto (global) Ct threshold method. Limit of detection (LOD) was set to a Ct of 28. The quality threshold was set to 0.65. Cts for qPCR reactions that failed the quality threshold (melting curves with deviating Tm temperatures) were converted to 28. The Ct values were then exported to Excel and converted to expression levels using the equation Log Ex = Ct[LOD]-Ct[Assay]. The expressions of *Actb* and *Tbp* housekeeping genes were measured to determine which sample actually contained a cell. Cells that fail to amplify systematically all the tested genes or to express germ cell markers (*Dazl*, *Ddx4* and *Kit*) were excluded from further analysis. The percentages of cells excluded was 23% at E13.5 and 34% at E14.5. This can be explained by the greater difficulty to isolate and collect germ cells at E14.5, compared to E13.5. The final analysis was done using n=68 individual cells at E13.5 (n=25 controls, n=43 mutants) and n=87 individual cells at E14.5 (n=40 controls, n=47 mutants). Results were not normalized relative to housekeeping genes, as their expression did not differ between control and mutant cells. Percentages of cells expressing a gene of interest are represented as histograms, and expression levels are represented as violin and box plot using R Studio software.

References

1 Borum, K. Oogenesis in the mouse. A study of the meiotic prophase. *Exp. Cell Res.* **24**, 495-507 (1961).

2 Drumond, A. L., Meistrich, M. L. & Chiarini-Garcia, H. Spermatogonial morphology and kinetics during testis development in mice: a high-resolution light microscopy approach. *Reproduction* **142**, 145-155 (2011).

3 McLaren, A. Germ cells and germ cell sex. *Philos. Trans. R. Soc. Lond. B Biol. Sci.* **350**, 229-233 (1995).

4 Byskov, A. G. & Saxen, L. Induction of meiosis in fetal mouse testis in vitro. *Dev. Biol*. **52**, 193-200 (1976).

5 Bowles, J. et al. Retinoid signaling determines germ cell fate in mice. *Science* **312**, 596-600 (2006).

6 Koubova, J. et al. Retinoic acid regulates sex-specific timing of meiotic initiation in mice. *Proc. Natl. Acad. Sci. USA* **103**, 2474-2479 (2006).

7 Kumar, S. et al. Sex-specific timing of meiotic initiation is regulated by Cyp26b1 independent of retinoic acid signalling. *Nat. Commun.* **2**, 151 (2011).

8 Bowles, J. et al. ALDH1A1 provides a source of meiosis-inducing retinoic acid in mouse fetal ovaries. *Nat. Commun.* **7**, 10845 (2016).

9 Duester, G. Involvement of alcohol dehydrogenase, short-chain dehydrogenase/reductase, aldehyde dehydrogenase, and cytochrome P450 in the control of retinoid signaling by activation of retinoic acid synthesis. *Biochemistry* **35**, 12221-12227 (1996).

10 Chambon, P. The nuclear receptor superfamily: a personal retrospect on the first two decades. *Mol. Endocrinol.* **19**, 1418-1428 (2005).

11 Al Tanoury, Z., Piskunov, A. & Rochette-Egly, C. Vitamin A and retinoid signaling: genomic and nongenomic effects. *J. Lipid Res.* **54**, 1761-1775 (2013).

12 Losel, R. & Wehling, M. Nongenomic actions of steroid hormones. *Nat. Rev. Mol. Cell Biol*. **4**, 46-56 (2003).

13 Bowles, J. & Koopman, P. Retinoic acid, meiosis and germ cell fate in mammals. *Development* **134**, 3401-3411 (2007).

14 Griswold, M. D., Hogarth, C. A., Bowles, J. & Koopman, P. Initiating meiosis: the case for retinoic acid. *Biol. Reprod.* **86**, 35 (2012).

15 Dolle, P., Ruberte, E., Leroy, P., Morriss-Kay, G. & Chambon, P. Retinoic acid receptors and cellular retinoid binding proteins. I. A systematic study of their differential pattern of transcription during mouse organogenesis. *Development* **110**, 1133-1151 (1990).

16 Jameson, S. A. et al. Temporal transcriptional profiling of somatic and germ cells reveals biased lineage priming of sexual fate in the fetal mouse gonad. *PLoS Genet.* **8**, e1002575 (2012).

17 Ruberte, E. et al. Specific spatial and temporal distribution of retinoic acid receptor gamma transcripts during mouse embryogenesis. *Development* **108**, 213-222 (1990).

18 Vernet, N. et al. Retinoic acid metabolism and signaling pathways in the adult and developing mouse testis. *Endocrinology* **147**, 96-110 (2006).

19 Wendling, O., Ghyselinck, N. B., Chambon, P. & Mark, M. Roles of retinoic acid receptors in early embryonic morphogenesis and hindbrain patterning. *Development* **128**, 2031-2038 (2001).

20 Yuan, L. et al. The synaptonemal complex protein SCP3 can form multistranded, cross-striated fibers in vivo. *J. Cell Biol.* **142**, 331-339 (1998).

21 Eijpe, M., Offenberg, H., Jessberger, R., Revenkova, E. & Heyting, C. Meiotic cohesin REC8 marks the axial elements of rat synaptonemal complexes before cohesins SMC1beta and SMC3. *J. Cell Biol.* **160**, 657-670 (2003).

22 Soh, Y. Q. et al. A Gene Regulatory Program for Meiotic Prophase in the Fetal Ovary. *PLoS Genet.* **11**, e1005531 (2015).

23 Baltus, A. E. et al. In germ cells of mouse embryonic ovaries, the decision to enter meiosis precedes premeiotic DNA replication. *Nat. Genet.* **38**, 1430-1434 (2006).

24 Mark, M., Ghyselinck, N. B. & Chambon, P. Function of retinoid nuclear receptors: lessons from genetic and pharmacological dissections of the retinoic acid signaling pathway during mouse embryogenesis. *Annu. Rev. Pharmacol. Toxicol.* **46**, 451-480 (2006).

25 Lohnes, D. et al. Function of the retinoic acid receptors (RARs) during development (I). Craniofacial and skeletal abnormalities in RAR double mutants. *Development* **120**, 2723-2748 (1994).

26 Bowles, J. et al. Retinoic Acid Antagonizes Testis Development in Mice. *Cell Rep.* **24**, 1330-1341 (2018).

27 Koshimizu, U., Watanabe, M. & Nakatsuji, N. Retinoic acid is a potent growth activator of mouse primordial germ cells in vitro. *Dev. Biol.* **168**, 683-685 (1995).

28 Tedesco, M., Desimio, M. G., Klinger, F. G., De Felici, M. & Farini, D. Minimal concentrations of retinoic acid induce stimulation by retinoic acid 8 and promote entry into meiosis in isolated pregonadal and gonadal mouse primordial germ cells. *Biol. Reprod.* **88**, 145 (2013).

29 Koubova, J. et al. Retinoic acid activates two pathways required for meiosis in mice. *PLoS Genet.* **10**, e1004541 (2014).

30 Menke, D. B., Koubova, J. & Page, D. C. Sexual differentiation of germ cells in XX mouse gonads occurs in an anterior-to-posterior wave. *Dev. Biol.* **262**, 303-312 (2003).

31 Agrimson, K. S. & Hogarth, C. A. Germ Cell Commitment to Oogenic Versus Spermatogenic Pathway: The Role of Retinoic Acid. *Results Probl. Cell Differ.* **58**, 135-166 (2016).

32 Bowles, J. & Koopman, P. Sex determination in mammalian germ cells: extrinsic versus intrinsic factors. *Reproduction* **139**, 943-958 (2010).

33 Bowles, J. & Koopman, P. Precious cargo: regulation of sex-specific germ cell development in mice. *Sex Dev.* **7**, 46-60 (2013).

34 Feng, C. W., Bowles, J. & Koopman, P. Control of mammalian germ cell entry into meiosis. *Mol. Cell. Endocrinol.* **382**, 488-497 (2014).

35 Spiller, C. & Bowles, J. Sexually dimorphic germ cell identity in mammals. *Curr. Top. Dev. Biol.* **134**, 253-288 (2019).

36 Spiller, C. M., Bowles, J. & Koopman, P. Regulation of germ cell meiosis in the fetal ovary. *Int. J. Dev. Biol.* **56**, 779-787 (2012).

37 Kumar, S., Cunningham, T. J. & Duester, G. Resolving molecular events in the regulation of meiosis in male and female germ cells. *Sci. Signal* **6**, pe25 (2013).

38 Mu, X. et al. Retinoic acid derived from the fetal ovary initiates meiosis in mouse germ cells. *J. Cell Physiol.* **228**, 627-639 (2013).

39 Le Bouffant, R. et al. Msx1 and Msx2 promote meiosis initiation. *Development* **138**, 5393-5402 (2011).

40 Krentz, A. D. et al. DMRT1 promotes oogenesis by transcriptional activation of Stra8 in the mammalian fetal ovary. *Dev. Biol.* **356**, 63-70 (2011).

41 Miyauchi, H. et al. Bone morphogenetic protein and retinoic acid synergistically specify female germ-cell fate in mice. *EMBO J.* **36**, 3100-3119 (2017).

42 Liang, G. J. et al. Activin A accelerates the progression of fetal oocytes throughout meiosis and early oogenesis in the mouse. *Stem Cells Dev.* **24**, 2455-2465 (2015).

43 Wang, N. & Tilly, J. L. Epigenetic status determines germ cell meiotic commitment in embryonic and postnatal mammalian gonads. *Cell Cycle* **9**, 339-349 (2010).

44 Yokobayashi, S. et al. PRC1 coordinates timing of sexual differentiation of female primordial germ cells. *Nature* **495**, 236-240 (2013).

45 Dokshin, G. A., Baltus, A. E., Eppig, J. J. & Page, D. C. Oocyte differentiation is genetically dissociable from meiosis in mice. *Nat. Genet.* **45**, 877-883 (2013).

475 46 Tan, N. S. et al. Selective cooperation between fatty acid binding proteins and
476 peroxisome proliferator-activated receptors in regulating transcription. *Mol. Cell.*
477 *Biol*. **22**, 5114-5127 (2002).

478 47 Dong, D., Ruuska, S. E., Levinthal, D. J. & Noy, N. Distinct roles for cellular
479 retinoic acid-binding proteins I and II in regulating signaling by retinoic acid. *J.*
480 *Biol. Chem.* **274**, 23695-23698 (1999).

481 48 Sussman, F. & de Lera, A. R. Ligand recognition by RAR and RXR receptors:
482 binding and selectivity. *J. Med. Chem.* **48**, 6212-6219 (2005).

483 49 Barak, Y. et al. Effects of peroxisome proliferator-activated receptor delta on
484 placentation, adiposity, and colorectal cancer. *Proc. Natl. Acad. Sci. USA* **99**,
485 303-308 (2002).

486 50 Peters, J. M. et al. Growth, adipose, brain, and skin alterations resulting from
487 targeted disruption of the mouse peroxisome proliferator-activated receptor
488 beta(delta). *Mol. Cell. Biol.* **20**, 5119-5128 (2000).

489 51 Kruse, S. W. et al. Identification of COUP-TFII orphan nuclear receptor as a
490 retinoic acid-activated receptor. *PLoS Biol.* **6**, e227 (2008).

491 52 Zhou, X. E. et al. The orphan nuclear receptor TR4 is a vitamin A-activated
492 nuclear receptor. *J. Biol. Chem.* **286**, 2877-2885 (2011).

493 53 Andre, E. et al. Disruption of retinoid-related orphan receptor beta changes
494 circadian behavior, causes retinal degeneration and leads to vacillans phenotype
495 in mice. *EMBO J.* **17**, 3867-3877 (1998).

496 54 Persaud, S. D. et al. All trans-retinoic acid analogs promote cancer cell apoptosis
497 through non-genomic Crabp1 mediating ERK1/2 phosphorylation. *Sci. Rep.* **6**,
498 22396 (2016).

499 55 de Bruijn, D. R. et al. Normal development, growth and reproduction in cellular
500 retinoic acid binding protein-I (CRABPI) null mutant mice. *Differentiation* **58**, 141-
501 148 (1994).

502 56 Gorry, P. et al. The cellular retinoic acid binding protein I is dispensable. *Proc.*
503 *Natl. Acad. Sci. USA* **91**, 9032-9036 (1994).

504 57 Lampron, C. et al. Mice deficient in cellular retinoic acid binding protein II
505 (CRABPII) or in both CRABPI and CRABPII are essentially normal. *Development*
506 **121**, 539-548 (1995).

507 58 Teletin, M. et al. Two functionally redundant sources of retinoic acid secure
508 spermatogonia differentiation in the seminiferous epithelium. *Development* **146**,
509 pii: dev170225 (2019).

510 59 Germain, P. et al. Differential action on coregulator interaction defines inverse
511 retinoid agonists and neutral antagonists. *Chem. Biol.* **16**, 479-489 (2009).

60 Germain, P., Iyer, J., Zechel, C. & Gronemeyer, H. Co-regulator recruitment and the mechanism of retinoic acid receptor synergy. *Nature* **415**, 187-192 (2002).

61 Klein, E. S. et al. Identification and functional separation of retinoic acid receptor neutral antagonists and inverse agonists. *J. Biol. Chem.* **271**, 22692-22696 (1996).

62 Klein, E. S., Wang, J. W., Khalifa, B., Gavigan, S. A. & Chandraratna, R. A. Recruitment of nuclear receptor corepressor and coactivator to the retinoic acid receptor by retinoid ligands. Influence of DNA-heterodimer interactions. *J. Biol. Chem.* **275**, 19401-19408 (2000).

63 Chatagnon, A. et al. RAR/RXR binding dynamics distinguish pluripotency from differentiation associated cis-regulatory elements. *Nucleic Acids Res.* **43**, 4833-4854 (2015).

64 Giuili, G. et al. Murine spermatogonial stem cells: targeted transgene expression and purification in an active state. *EMBO Rep.* **3**, 753-759 (2002).

65 Rosenfeld, M. G., Lunyak, V. V. & Glass, C. K. Sensors and signals: a coactivator/corepressor/epigenetic code for integrating signal-dependent programs of transcriptional response. *Genes Dev.* **20**, 1405-1428 (2006).

66 Mahony, S. et al. Ligand-dependent dynamics of retinoic acid receptor binding during early neurogenesis. *Genome Biol.* **12**, R2 (2011).

67 Cunningham, T. J. & Duester, G. Mechanisms of retinoic acid signalling and its roles in organ and limb development. *Nat. Rev. Mol. Cell Biol.* **16**, 110-123 (2015).

68 Ghyselinck, N. B. & Duester, G. Retinoic acid signaling pathways. *Development* **146**, pii: dev167502 (2019).

69 Horton, C. & Maden, M. Endogenous distribution of retinoids during normal development and teratogenesis in the mouse embryo. *Dev. Dyn.* **202**, 312-323 (1995).

70 Livera, G., Rouiller-Fabre, V., Valla, J. & Habert, R. Effects of retinoids on the meiosis in the fetal rat ovary in culture. *Mol. Cell. Endocrinol.* **165**, 225-231 (2000).

71 Kocer, A., Reichmann, J., Best, D. & Adams, I. R. Germ cell sex determination in mammals. *Mol. Hum. Reprod.* **15**, 205-213 (2009).

72 McLaren, A. & Southee, D. Entry of mouse embryonic germ cells into meiosis. *Dev. Biol.* **187**, 107-113 (1997).

73 MacLean, G., Li, H., Metzger, D., Chambon, P. & Petkovich, M. Apoptotic extinction of germ cells in testes of Cyp26b1 knockout mice. *Endocrinology* **148**, 4560-4567 (2007).

74 Chapellier, B. et al. A conditional floxed (loxP-flanked) allele for the retinoic acid receptor alpha (RARalpha) gene. *Genesis* **32**, 87-90 (2002).

549 75 Chapellier, B. et al. A conditional floxed (loxP-flanked) allele for the retinoic acid
550 receptor gamma (RARgamma) gene. *Genesis* **32**, 95-98 (2002).

551 76 Chapellier, B. et al. A conditional floxed (loxP-flanked) allele for the retinoic acid
552 receptor beta (RARbeta) gene. *Genesis* **32**, 91-94 (2002).

553 77 Ghyselinck, N. B. et al. Role of the retinoic acid receptor beta (RARbeta) during
554 mouse development. *Int. J. Dev. Biol.* **41**, 425-447 (1997).

555 78 Ruzankina, Y. et al. Deletion of the developmentally essential gene ATR in adult
556 mice leads to age-related phenotypes and stem cell loss. *Cell Stem Cell* **1**, 113-
557 126 (2007).

558 79 Muzumdar, M. D., Tasic, B., Miyamichi, K., Li, L. & Luo, L. A global double-
559 fluorescent Cre reporter mouse. *Genesis* **45**, 593-605 (2007).

560 80 De Felici, M. & McLaren, A. Isolation of mouse primordial germ cells. *Exp. Cell*
561 *Res.* **142**, 476-482 (1982).

562 81 Adams, I. R. & McLaren, A. Sexually dimorphic development of mouse primordial
563 germ cells: switching from oogenesis to spermatogenesis. *Development* **129**,
564 1155-1164 (2002).

Acknowledgments

We thank Dr Amandine Chassot, Dr Marie-Christine Chaboissier and Dr Eric Pailhoux for discussions, advices and critical reading of the manuscript. We also thank Dr Christelle Thibault-Carpentier from the Genomeast platform for her input (http://genomeast.igbmc.fr/). This work was supported by grants from CNRS, INSERM, UNISTRA and Agence Nationale pour la Recherche (ANR; 10-BLAN-1239, 13-BSV6-0003 and 13-BSV2-0017), as well as from EU (FP7-PEOPLE-IEF-2012-331687). Their studies were also supported in part by the grant ANR-10-LABX-0030-INRT, a French State fund managed by the ANR under the frame programme Investissements d'Avenir labelled ANR-10-IDEX-0002-02.

Author contributions

N.V., M.M., and N.B.G. designed the study, analyzed the data and wrote the paper. N.V., M.M., D.C., B.F., M.K., V.A. and M.T. performed the experiments, analyzed the data, and discussed the results. M.T. additionally commented on the manuscript.

Additional information

Supplementary Information accompanies his paper.

Competing financial interests: The authors declare no competing financial interests.

Word count: 3136

Figure Legends

Fig. 1. Expression of RARs in the female gonad and germ cells during embryonic development. (A and B) Immunohistochemical detection of RARA and RARG (red signals) on frontal histological sections of a E11.5 wild-type female embryo: expression of RARG is confined to the precartilaginous anlage of a vertebra, while that of RARA is more widespread and includes notably the undifferentiated gonad. (B') Same section as (B) stained with hematoxylin and eosin. (C-E) Enlargement of the box in (A): RARA (in red) is detected in the nuclei of some somatic cells of the gonad (arrowheads) and of the coelomic epithelium; in contrast, the large, rounded nuclei characteristic of germ cells (arrows) do not exhibit anti-RARA immunostaining. Nuclei are counterstained with DAPI (blue signal). Ao; aorta; CE, coelomic epithelium; Go, gonad; Me, mesonephros; SC, spinal cord; V, vertebra; Scale bar (in E): 160 µm (A,B,B') and 30 µm (C-E). (F,G) RT-qPCR analysis comparing the expression levels and distributions of the germ cell markers *Dazl*, *Ddx4* and *Kit* (F) and *Rara*, *Rarb* and *Rarg* (G) mRNAs in single germ cells from control and mutant ovaries at E13.5 and E14.5. The Violin plot width and length represent respectively the number of cells and the range of expression (Log2Ex). The box-and-whisker plots illustrate medians, ranges and variabilities of the collected data. The histograms show the percentages of expressing cells in each group. At respectively E13.5 and E14.5, *Rara* is present in 96% and 83% of germ cells; *Rarb* in none of germ cells since the fetus are on a *Rarb*-null genetic background (see Methods); *Rarg* is present in 84% and 65% of germ cells. Importantly, *Rara*, *Rarb* and *Rarg* are undetectable in germ cells isolated from the *Rar*-mutant ovaries (see main text for details).

Fig. 2. Markers of meiotic prophase I are robustly expressed at E14.5 in ovaries of mutants lacking RARs. (A) Detection of meiotic cells expressing SYCP3 (green nuclear signal), REC8 or STRA8 (red nuclear signals) on consecutive, 5 µm thick, transverse histological sections at four different levels of the ovaries from control and mutant fetuses, as indicated. DDX4 (red cytoplasmic signal) is present in all germ cells. The positions of histological sections along the anteroposterior axis is indicated in terms of distance from the anterior pole of the ovary (i.e., 50, 200, 350 and 500 microns). + 5 µm and + 10 µm: the indicated histological sections "REC8" and "STRA8" on each line are, respectively, 5 and 10 microns apart from the indicated section "DDX4 + SYCP3" that was used to establish the total number of germ cells. Nuclei are counterstained with DAPI (blue signal). Scale bar: 60 µm. (B) Average of the total number of germ cells present at the 4 different levels of the ovary illustrated in panel A in 4 control (white bars) and 4 mutant (grey bars) fetuses at E14.5. (C) Mean percentages of germ cells expressing SYCP3, REC8 and STRA8 in 4 control (white bars) and 4 mutant (grey bars) fetuses at E14.5. The asterisk (in C) indicates a significant difference ($p<0.05$).

Fig. 3. Evidence that gene excision has actually occurred in meiotic cells 4 days after administration of TAM. (A-F) Detection of the meiotic markers SYCP3, REC8 or STRA8 (red nuclear signals) and of mGFP (green membranous signal) on consecutive, 5 µm thick, transverse histological sections at two different levels of the ovary of a mutant fetus at E14.5. Efficient excision of the reporter transgene by cre/ERT^2 is assessed by mGFP expression in virtually all meiotic germ cells. Possible exceptions (i.e, red nuclei without a green contour) are indicated by white arrowheads. The position of histological sections along the anteroposterior axis is indicated on the left side in terms of distance from the anterior pole of the ovary (i.e., 200 and 350

631 microns). + 5 µm and + 10 µm: the indicated histological sections “REC8 + mGFP” and
632 “STRA8 + mGFP” on each line are, respectively, 5 and 10 microns apart from the
633 indicated section “SYCP3 + mGFP”. Nuclei are counterstained with DAPI (blue signal).
634 Scale bar (F): 60 µm. (G,H) PCR analysis of genomic DNA extracted from ovaries of
635 control and mutant fetuses at E13.5, as indicated. (G) DNA was genotyped using
636 primers 5’-CAGGGAGGATGCTGTTTGTA-3’, 5’- AACTGCTGCTCTGGGTCTC G-3’
637 and 5’-TACACTAACTACCCTTGACC-3’ to amplify the *Rara* wild-type (+, 371 bp-long),
638 the *Rara* L2 allele (427 bp-long), and the *Rara* L- (357 bp long) alleles. (H) DNA was
639 genotyped using primers 5’-TGCTTAGCATACTTGAGAAC-3’, 5’-ACCGCACGAC
640 ACGATAGGAC-3’ and 5’-GTAGATGCTGGGAATGGAAC-3’ to amplify the *Rarg* wild-
641 type (+, 707 bp-long), the *Rarg* L2 (768 bp-long) and the *Rarg* L- (495 bp-long) alleles.
642 (I) RT-qPCR analysis comparing the levels and distributions of *Sycp3*, *Rec8* and *Stra8*
643 mRNAs in single germ cells from control and mutant ovaries at E13.5 and E14.5. The
644 Violin plot width and length represent respectively the number of cells and the range
645 of expression (Log2Ex). The box-and-whisker plots illustrate medians, ranges and
646 variabilities of the collected data. The histograms show the percentages of expressing
647 cells in each group. *Sycp3*, *Rec8* and *Stra8* are present in 94%, 91% and 72% of
648 mutant germ cells at E14.5.

649 **Fig. 4. Mutant fetuses generated upon TAM injection at E9.5 display a spectrum**
650 **of congenital defects typically observed at E14.5 in compound RAR-knockout**
651 **mutants**. Frontal histological sections at similar levels of E14.5 control (A,C,E,G,I,K)
652 and mutant (B,D,F,H,J,L) female fetuses. (A,B) In mutants, the ventral portion of the
653 retina (vR) is reduced in size in comparison to the dorsal retina (dR), the lens (L) is
654 rotated ventrally and the eyelid folds (Ey) are fused together. (C,D) Mutants display
655 mesenchymal condensations indicating the position of the salivary glands (asterisks in

D), but their epithelial portion (SG in C) is absent. (E,F) In mutants, the thickness of the compact layer of the myocardium (green arrowheads) is markedly reduced in both right and left ventricles (rV and lV, respectively). (G,H) Mutants display hypoplasia of the right and left lungs (rL and lL, respectively). (I,J) Mutants, have hypoplastic kidneys (K). (K,L) Mutants lack the Müllerian duct (MD in K). Sections were stained with hematoxylin and eosin. H, heart; Me, mesonephros; Oe, oesophagus; Ov, ovary; PP, palatal process; SC, spinal cord; SG, salivary glands; T, tongue; V, vertebra; WD, Wolffian duct. Scale bar (in L): 160 µm (A,B), 320 µm (C,D,E,F,I,J), 640 µm (G,H) and 60 µm (K,L).

Fig. 5. All germ cells have entered meiosis at E15.5 in ovaries of mutants lacking RARs. (A,B) Detection of germ cells (DDX4-positive, red cytoplasmic signal) expressing SYCP3 (green nuclear signal): in both control (A) and mutant (B) ovaries, almost all germ cells express SYCP3 at high levels; exceptions (i.e, cells expressing SYCP3 at low to undetectable levels) are indicated by white arrowheads. (C,D) High power magnification views of germ cells immunostained for detection of SYCP1 (red signal) and SYCP3 (green signal): thread-like structures of only SYCP3 are characteristic of late leptotene stages (LL), while those containing also SYCP1 indicate zygotene stages (Z). (E-H) Detection of REC8 (red nuclear signal) or STRA8 (red nuclear signal): both control (E,G) and mutant (F,H) ovaries contain similar small numbers of germ cells expressing REC8 or STRA8. Note that (A,E,G) and (B,F,H) are adjacent longitudinal sections through the same control and mutant ovary, respectively. Nuclei are counterstained with DAPI (blue signal). Scale bar (in H): 60 µm (A,B,E-H) and 15 µm (C,D).

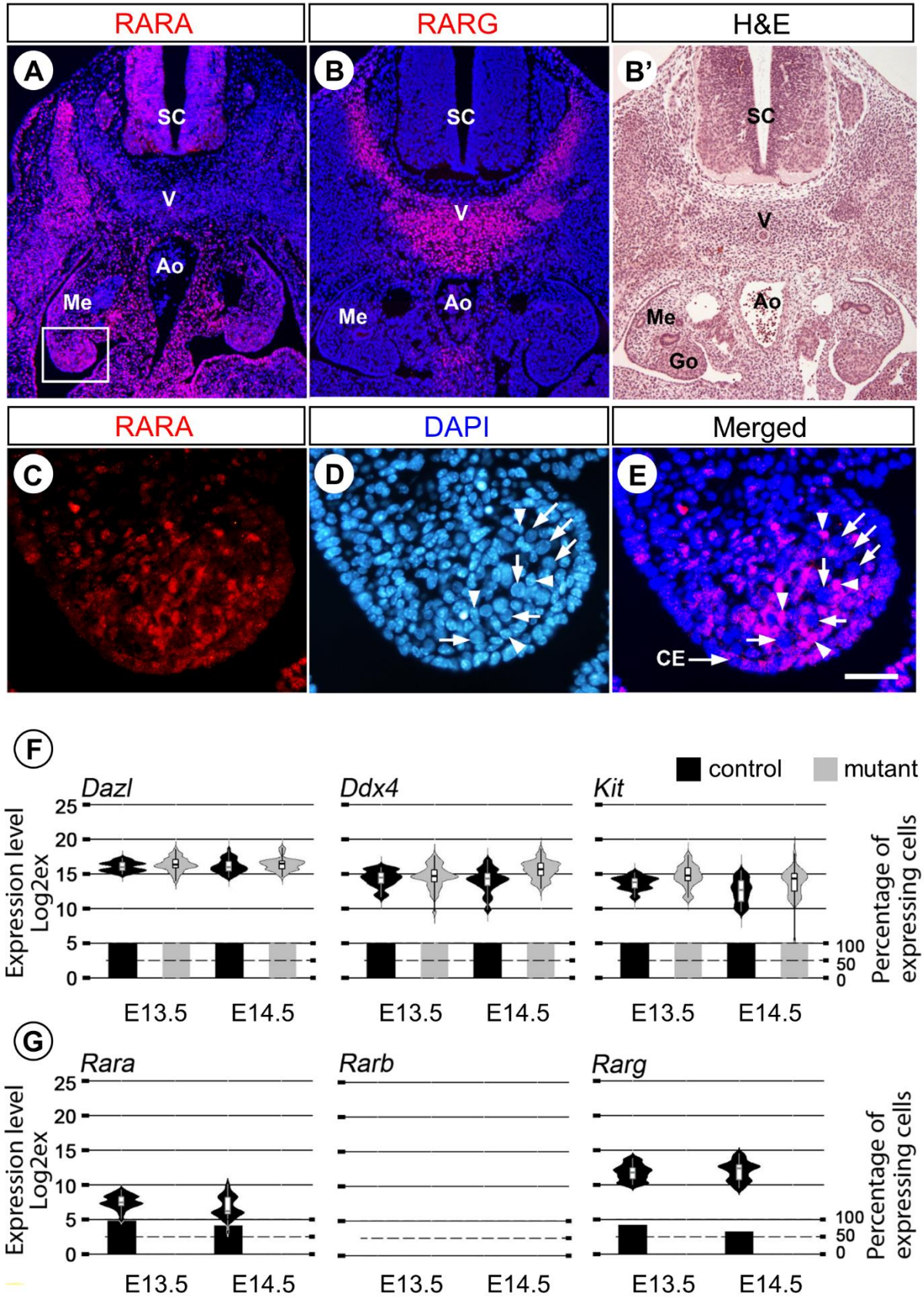

Figure 1

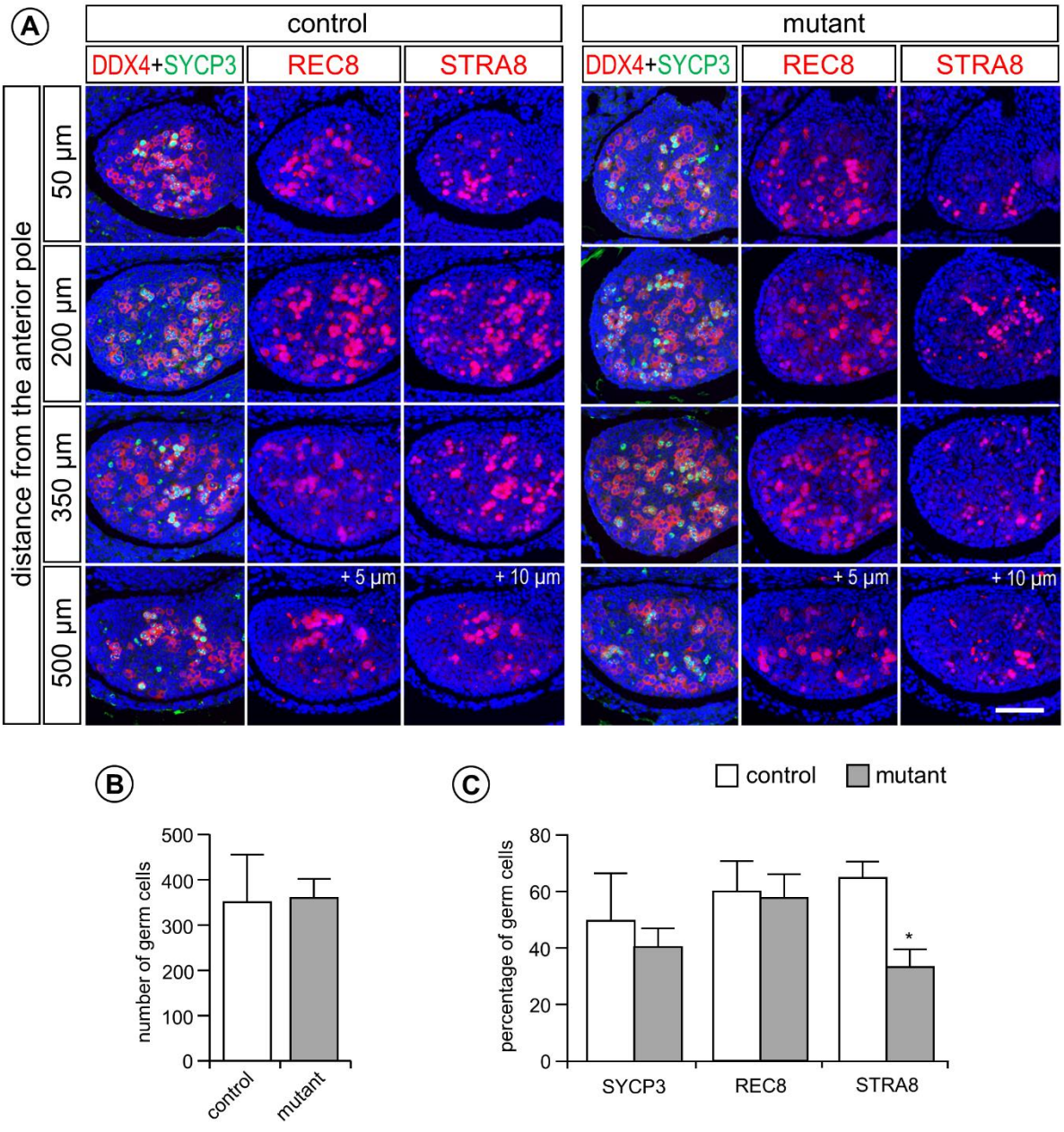

Figure 2

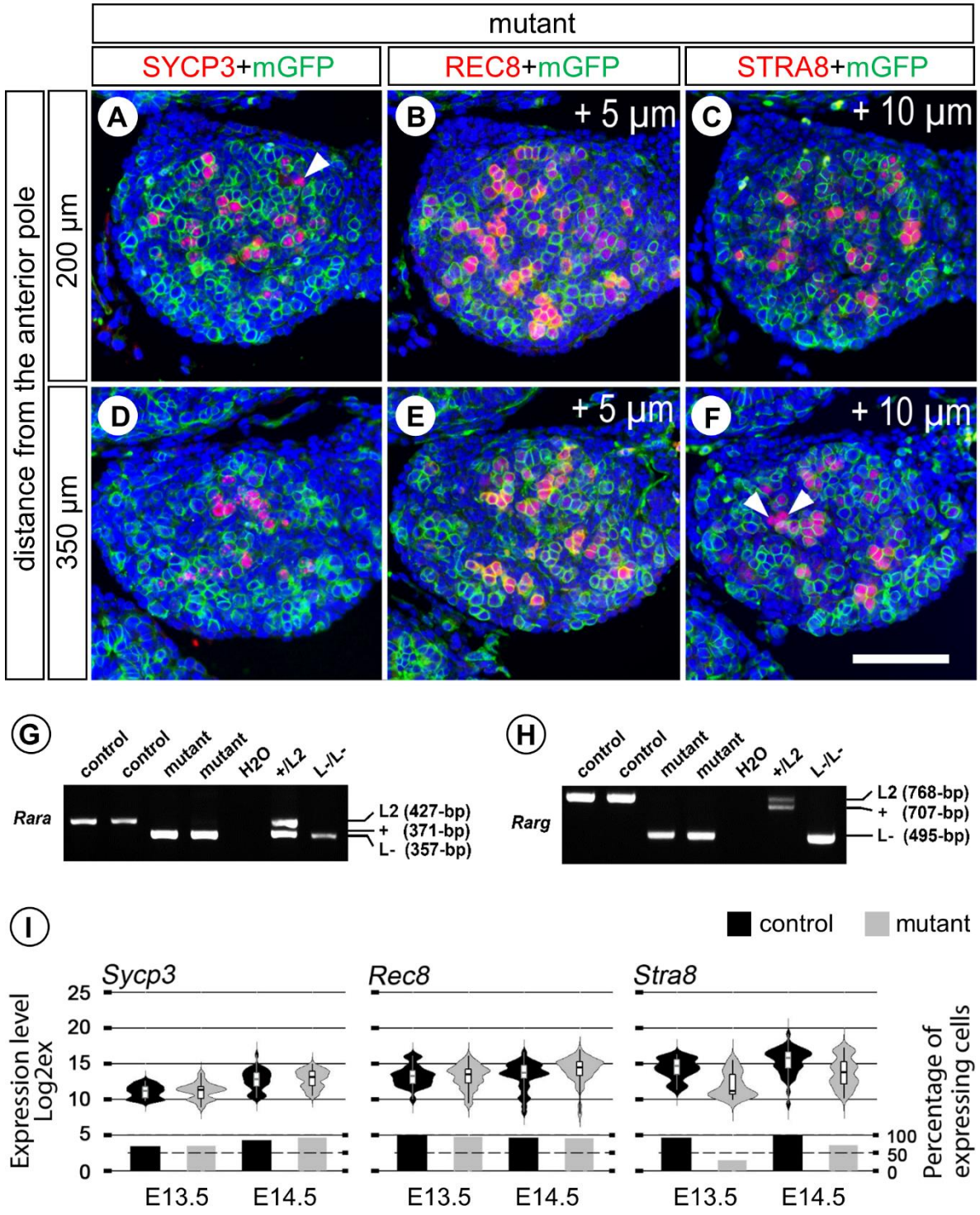

Figure 3

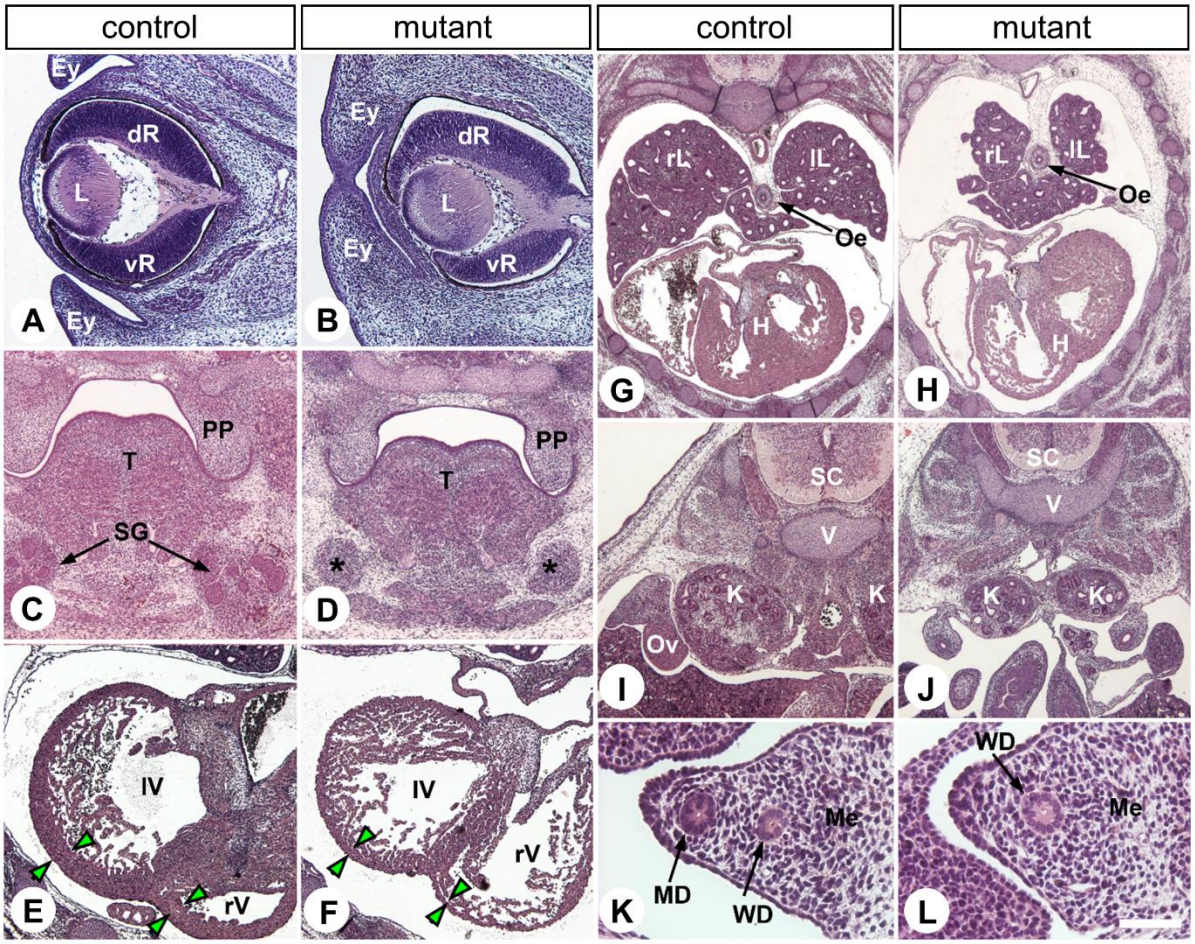

Figure 4

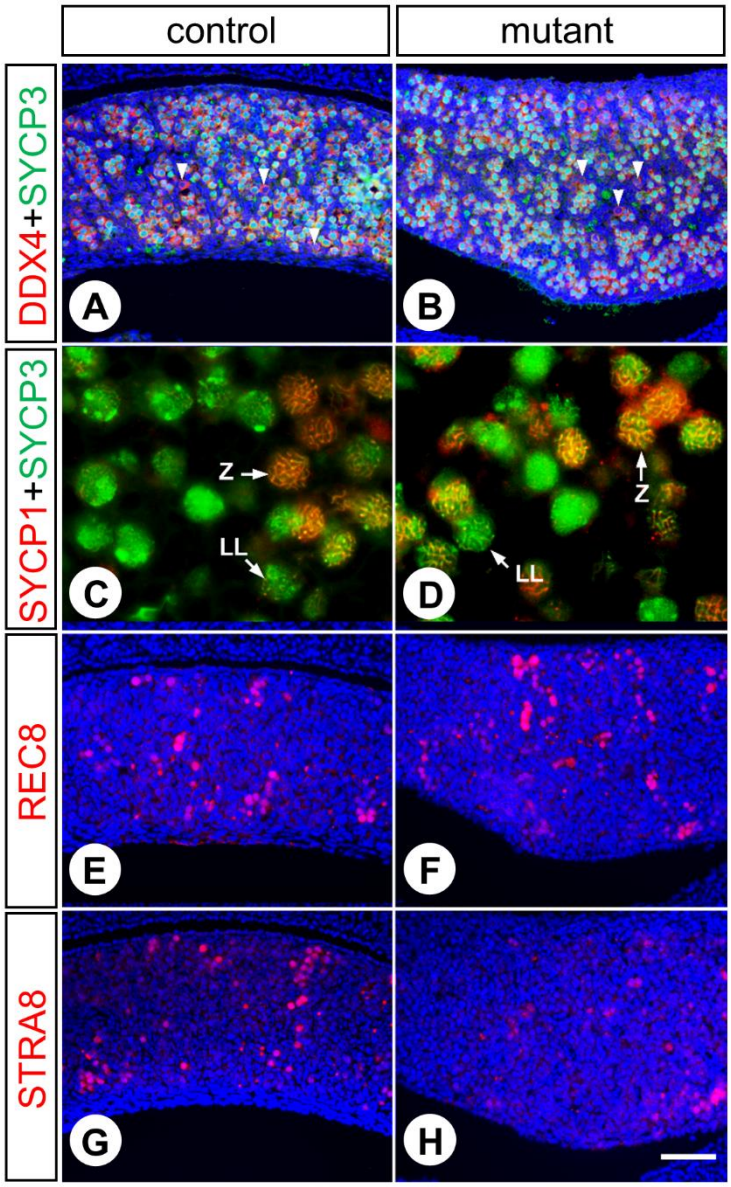

687

688 Figure 5

MEIOSIS INITIATES IN THE FETAL OVARY OF MICE LACKING ALL RETINOIC ACID RECEPTOR ISOTYPES

Nadège VERNET[1], Manuel MARK[1,2], Betty FÉRET[1], Muriel KLOPFENSTEIN[1], Diana CONDREA[1], Violaine ALUNNI[3], Marius TELETIN[1,2], and Norbert B. GHYSELINCK[1]

Supplementary Information

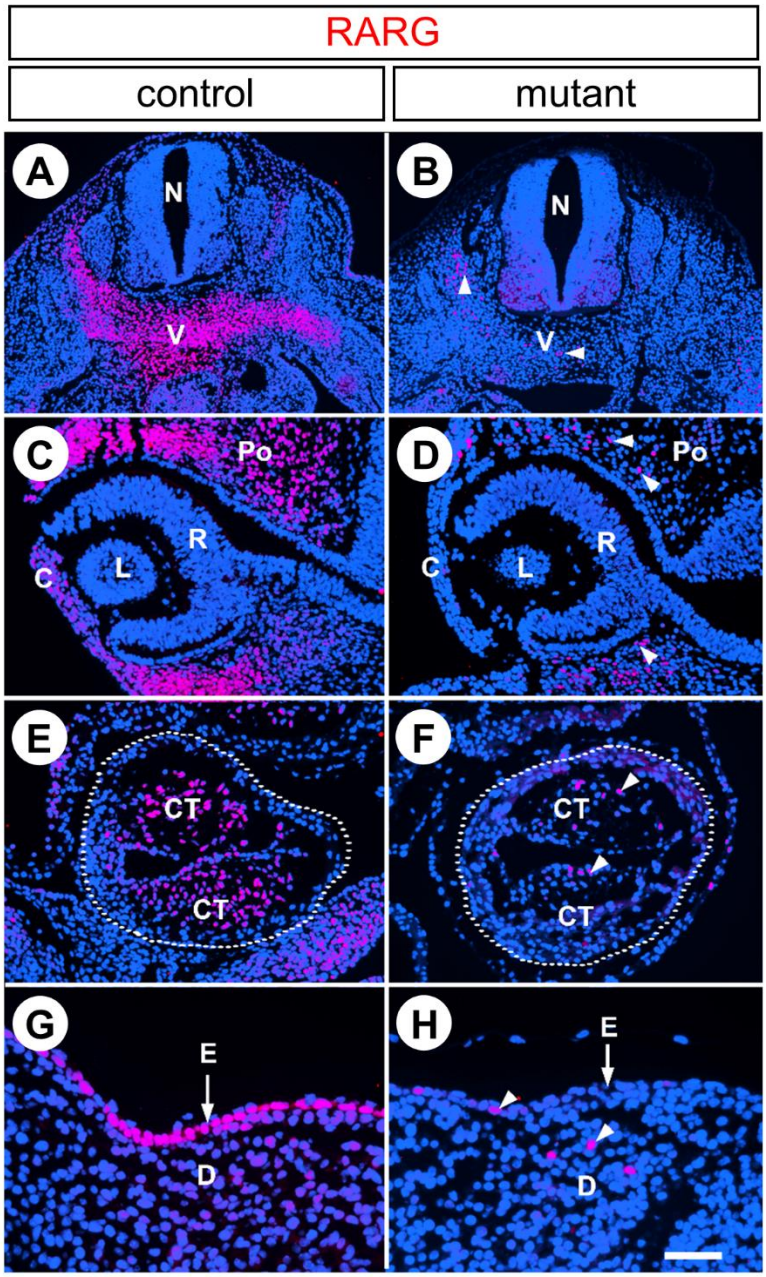

694

695 **Suppl. Fig. 1. Excision of RARG after administration of TAM at E10.5**.
696 immunohistochemical detection of RARG (red signal) on frontal histological sections
697 at similar levels of control and mutant embryos at E11.5, namely 24 hours after TAM
698 administration. (A,C,E,G) RARG is strongly expressed in precartilaginous vertebrae,
699 in periocular and corneal mesenchyme, in conotruncal ridges and in epidermis of the
700 control embryo. (B,D,F,H) Expression of RARG is nearly abolished in the tissues of the
701 mutant embryo. Nuclei are counterstained with DAPI (blue signal). C, cornea; CT,
702 conotruncal ridges; D, dermis; E, epidermis; L, lens; Po, periocular mesenchyme; R,
703 retina; V vertebra; The dotted lines mark off the periphery of the heart outflow tract.
704 White arrowheads indicate nuclei that are still expressing RARG in the mutant tissues.
705 Scale bar (in H): 160 µm (A,B), 80 µm (C-F) and 40 µm (G-H).

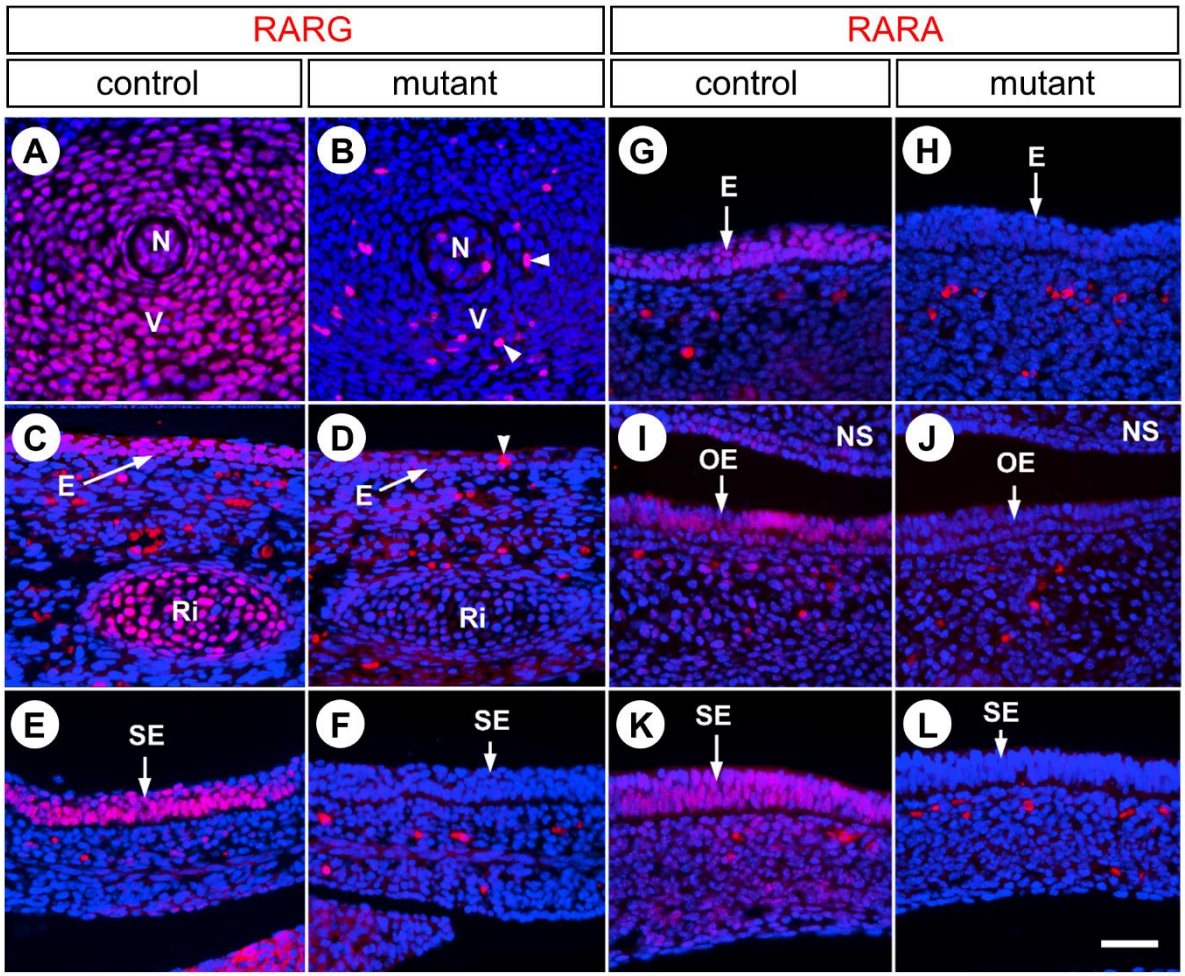

Suppl. Fig. 2. Excision of RARG and RARA after administration of TAM at E10.5. Immunohistochemical detection of RARG (red signal in A-F) and RARA (red signal in G-L) on histological sections of control and mutant fetuses at E14.5, namely 4 days after TAM administration. (A,C,E) RARG is strongly expressed in all cartilages including vertebrae (V) and ribs (Ri), as well as in the epidermis (E) and epithelium of the stomach (SE) of control fetuses. (B,D,F) Expression of RARG is abolished in almost all cells in tissues of mutant fetuses. (G,I,K) RARA is strongly expressed in the snout epidermis (E), olfactory epithelium (OE) and epithelium of the stomach (SE) of control fetuses. (H,J,L) Expression of RARA is lost in tissues of the mutant fetuses. Nuclei are counterstained with DAPI (blue signal). N, notochord; NS, nasal septum. White arrowheads indicate nuclei that are still expressing RARG in mutant tissues. Scale bar (in L): 40 µm (A-L).

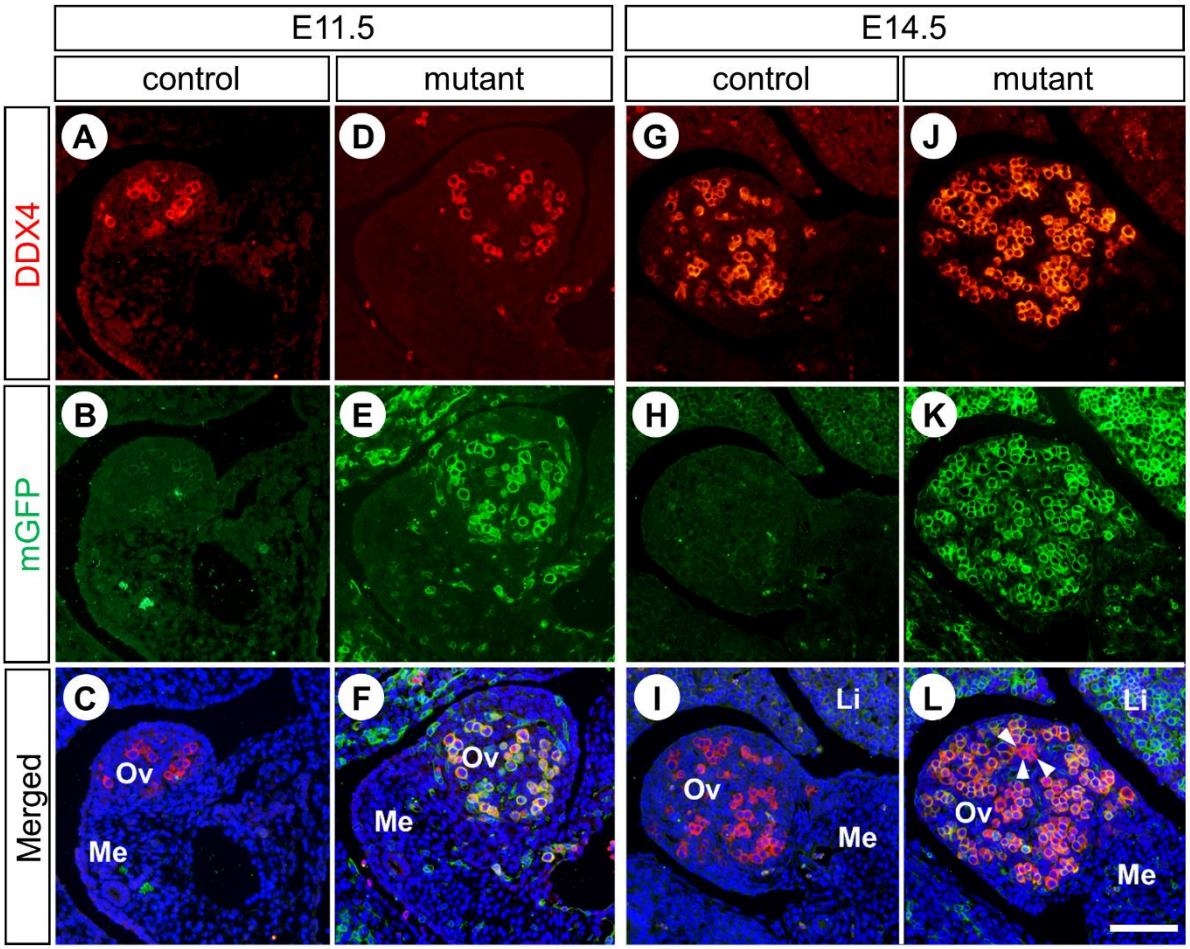

Suppl. Fig. 3. Excision of the *mT/mG* reporter in fetal ovaries after administration of TAM at E10.5. Detection of DDX4 (red cytoplasmic signal) and mGFP (green membranous signal) on histological sections of control and mutant ovaries at E11.5 (A-F) and E14.5 (G-L), namely 24 hours and 4 days after TAM administration, respectively. Efficient *mT/mG* excision is assessed by GFP expression in almost all germ cells (D-F and J-L); exceptions (i.e, red cytoplasm without a green contour) are indicated by white arrowheads. Most importantly, GFP is never detected in control ovaries, i.e., in the absence of cre/ERT^2 (A-C and G-I). Nuclei are counterstained with DAPI (blue signal). Li, Liver; Me, mesonephros; Ov, ovary. Scale bar (in L): 80 µm (A-L).

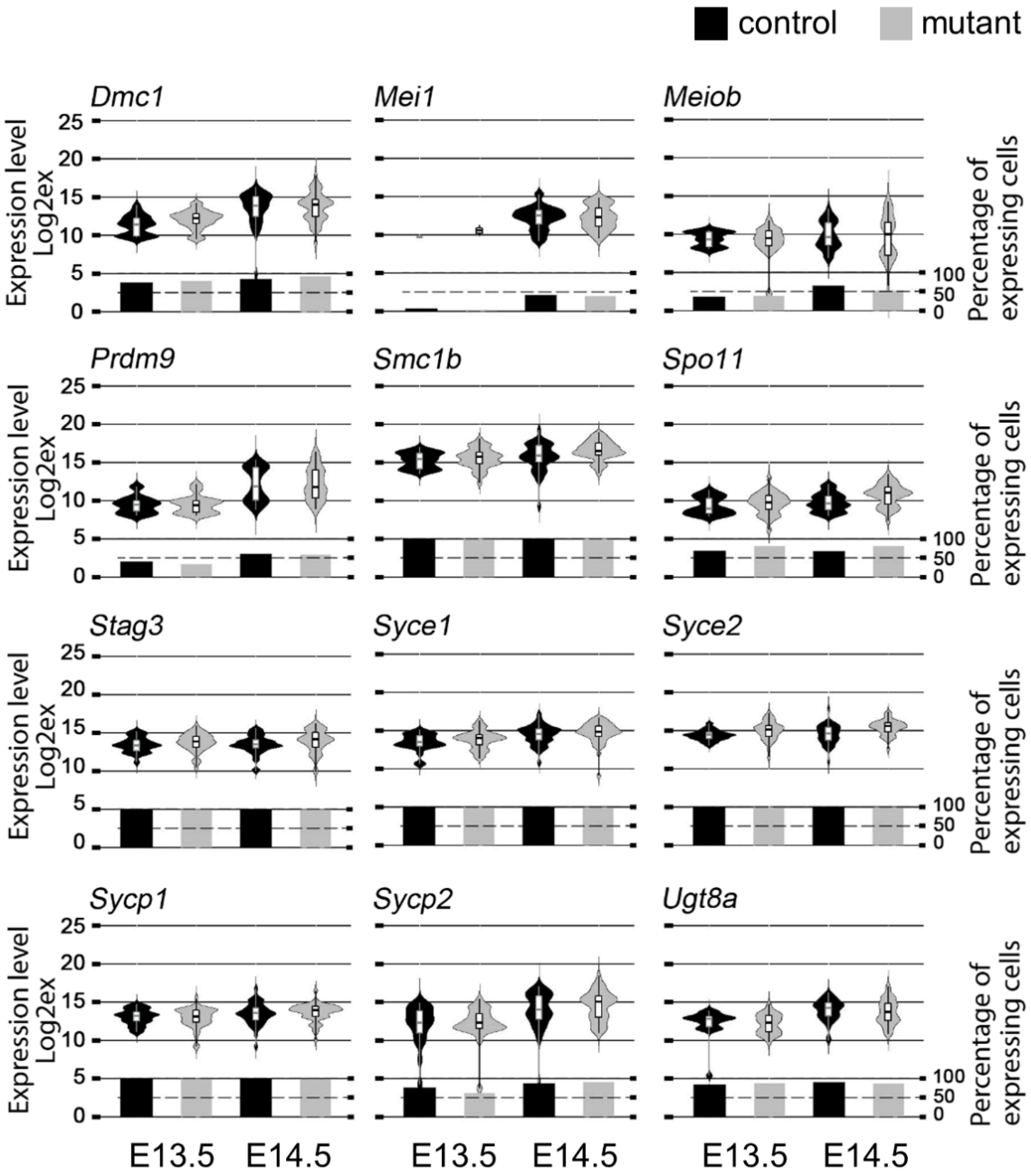

Suppl. Fig. 4. Meiotic genes are expressed at E13.5 and E14.5 in ovaries of mutant lacking RARs. RT-qPCR analysis comparing the levels and distributions of the meiotic markers *Dmc1*, *Mei1*, *Meiob*, *Prdm9*, *Smc1b*, *Spo11*, *Stag3*, *Syce1*, *Syce2*, *Sycp1*, *Sycp2* and *Ugt8a* mRNAs in single germ cells from control and mutant ovaries at E13.5 and E14.5. The Violin plot width and length represent respectively the number of cells and the range of expression (Log2Ex). The box-and-whisker plots illustrate medians, ranges and variabilities of the collected data. The histograms show the percentages of expressing cells in each group. A total of 155 cells were used for analysis (for see details, see Material and Methods).

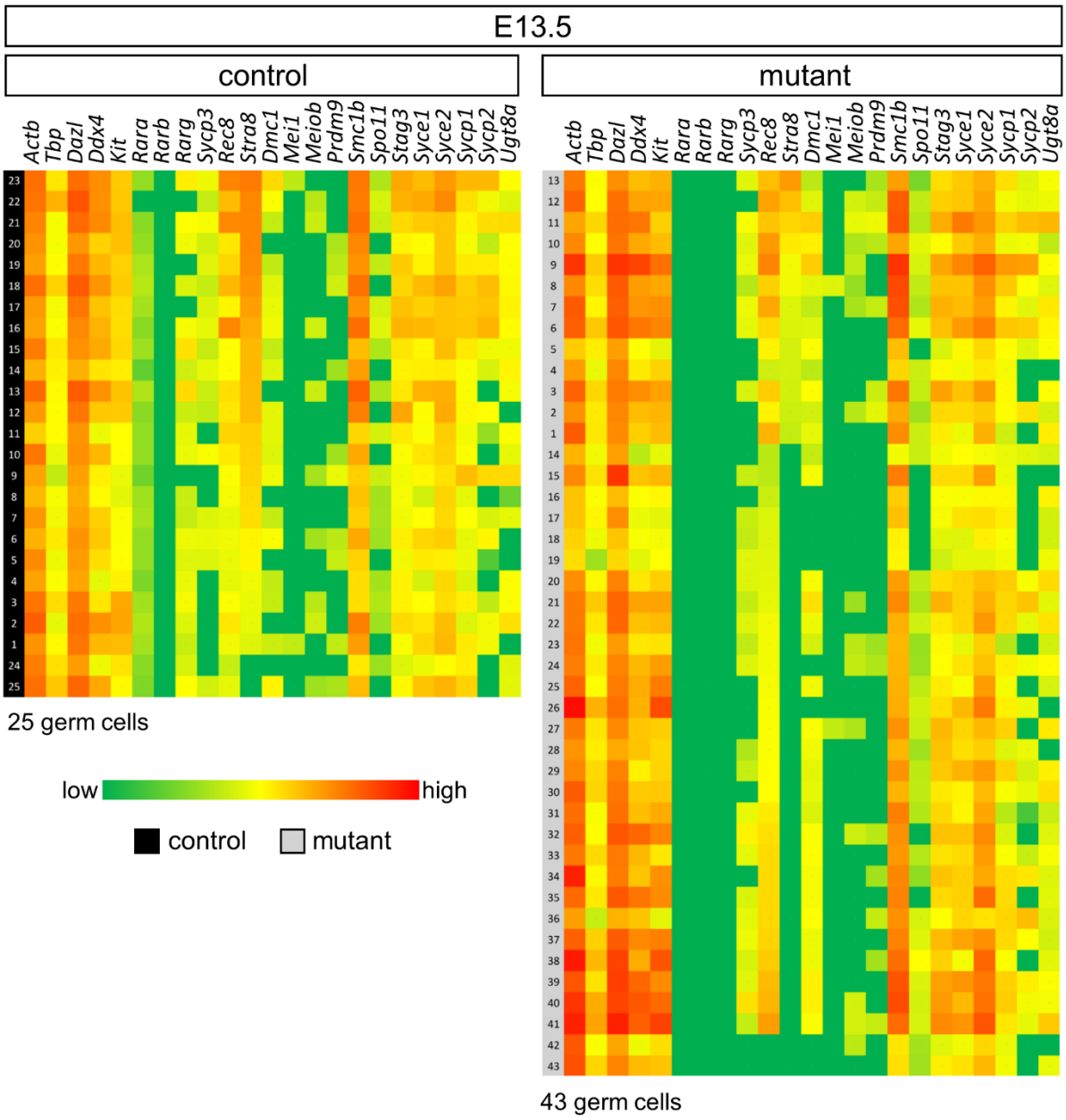

740 **Suppl. Fig. 5. Meiotic genes are expressed at E13.5 in ovaries of mutant lacking**
741 **RARs.** Heatmap showing the expression of 23 genes (columns) for each of the germ
742 cell analyzed (rows). Green, yellow and red indicate low, intermediate and high
743 expression levels, respectively. Cell clustering was based on the *Stra8* gene
744 expression pattern. Control cells are numbered 1 to 25 (black boxes), and mutant cells
745 are numbered 1 to 43 (grey boxes).

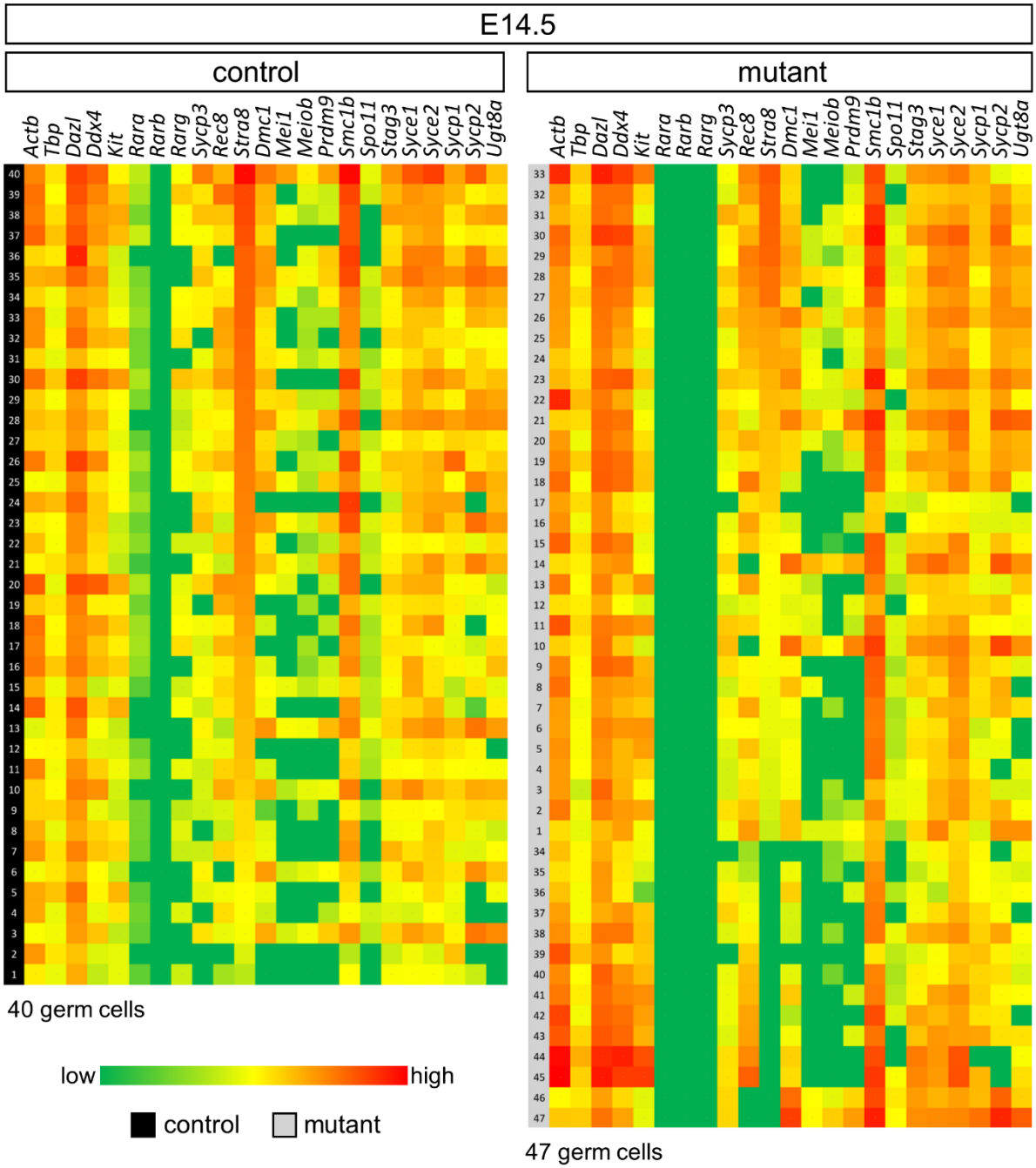

Suppl. Fig. 6. Meiotic genes are expressed at E14.5 in ovaries of mutant lacking RARs. Heatmap showing the expression of 23 genes (columns) for each of the germ cell analyzed (rows). Green, yellow and red indicate low, intermediate and high expression levels, respectively. Cell clustering was based on the Stra8 gene expression pattern. Control cells are numbered 1 to 40 (black boxes), and mutant cells are numbered 1 to 47 (grey boxes).

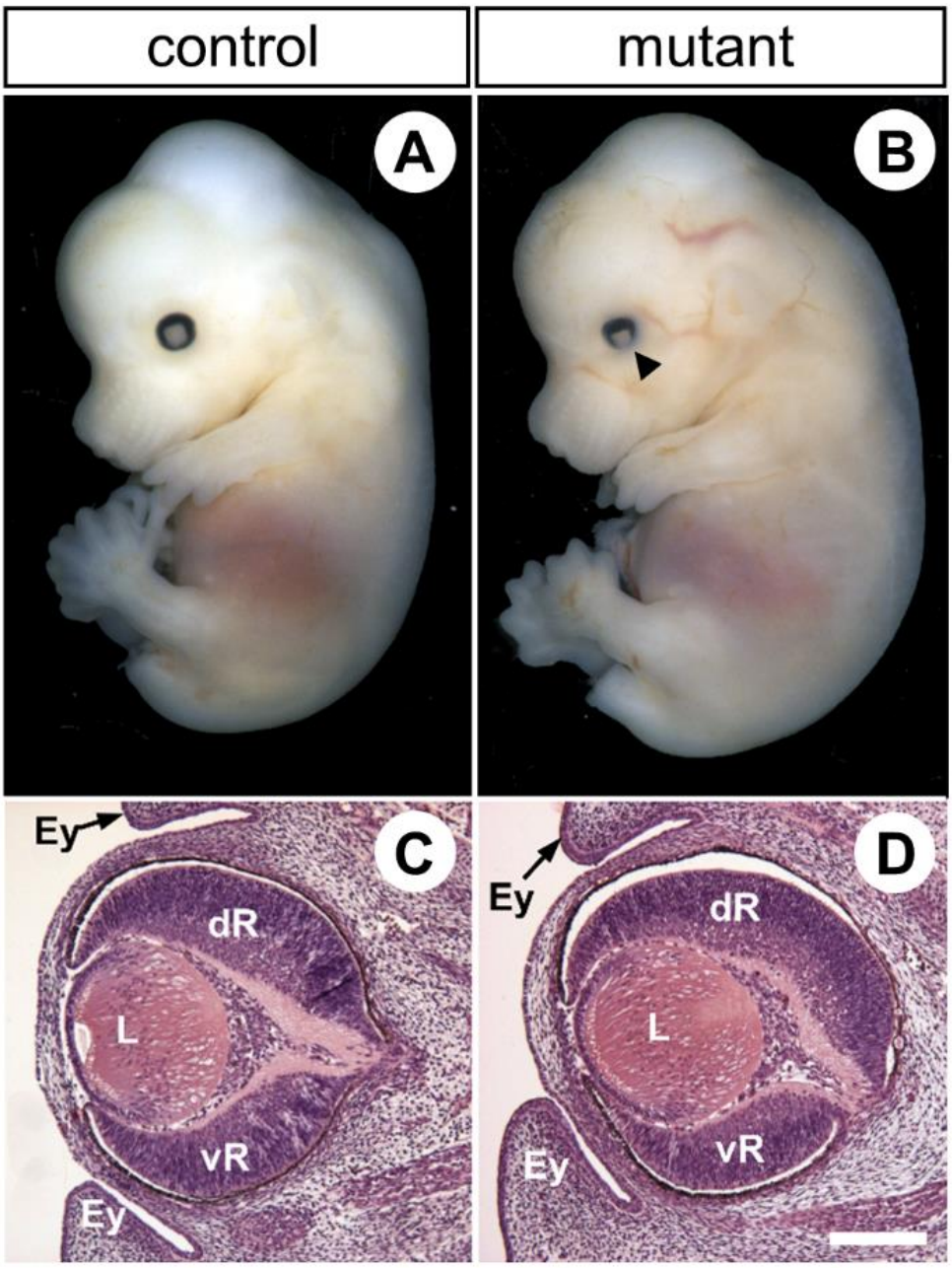

752

753 **Suppl. Fig. 7. Congenital malformations in E14.5 mutant fetuses generated upon**
754 **TAM injection at E10.5 are restricted to eye defects typically observed in RAR-**
755 **knockout mutants.** (A,B) The pigmented retina is externally less visible in the mutant
756 (arrowhead in B). This is because the insertions of the upper and lower eyelid folds
757 (Ey) are abnormally close to each other. (C,D) In the mutant, in addition to the closer
758 eyelid folds, the ventral portion of the retina (vR) is reduced in size in comparison to
759 the dorsal retina (dR) and the lens (L) is rotated ventrally. Histological sections were
760 stained with hematoxylin and eosin. Scale bar (in D): 160 µm (C,D).

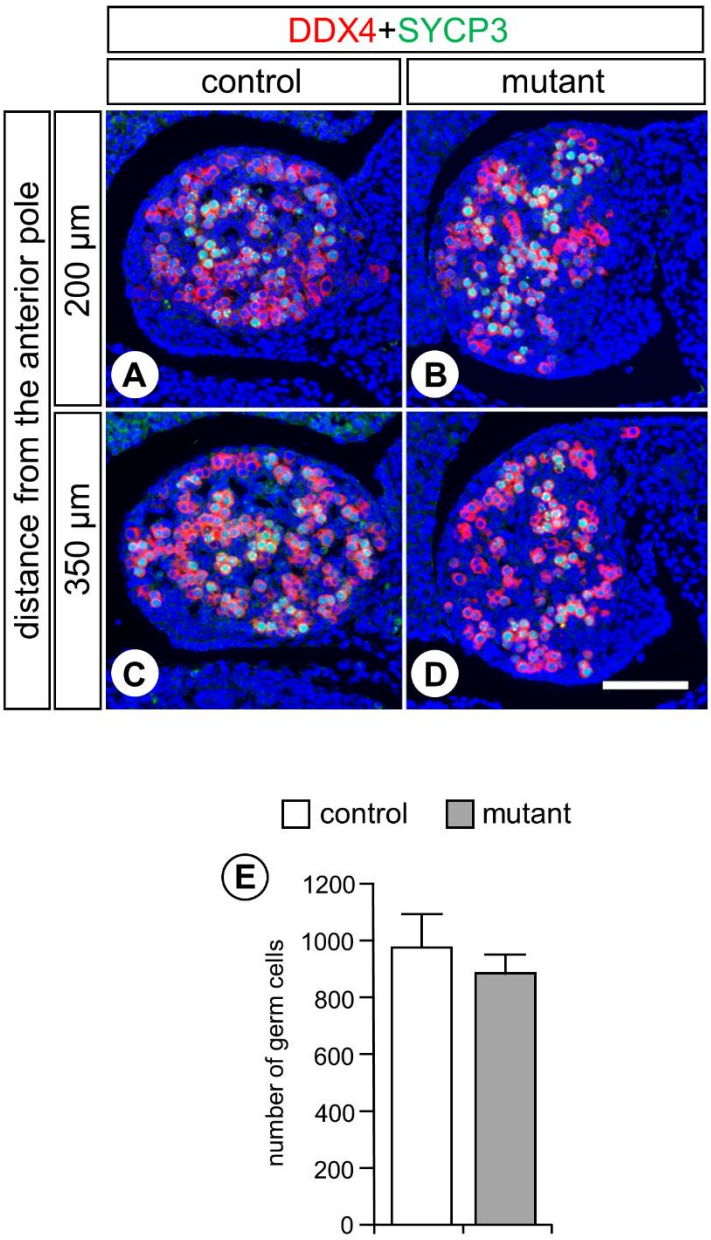

761 **Suppl. Fig. 8. Ovaries of mutants generated upon TAM injection at E9.5 display**
762 **a normal number of germ cells and contain meiotic cells.** (A-D) Detection of DDX4
763 (red cytoplasmic signal) and SYCP3 (green nuclear signal), on transverse histological
764 sections at two different levels of the ovaries from control and mutant fetuses at E14.5.
765 (A) and (C), and (B) and (D), are consecutive histological sections. The positions of
766 histological sections along the anteroposterior axis is indicated on the left in terms of
767 distance from the anterior pole of the ovary (i.e., 200 and 350 microns). Nuclei are
768 counterstained with DAPI (blue signal). Scale bar (in D): 60 µm. (E) Average of the
769 total number of germ cells present at the 7 different levels of the ovaries, 75 microns
770 apart, in 3 control (white bar) and 3 mutant fetuses (grey bar).

Antigen	Species	Reference	Source	Secondary antibody
DDX4	Rabbit	ab13840	Abcam	Cy3-conjugated donkey anti-rabbit IgG
mGFP	Chicken	GFP-1020	Aves	Alexa Fluor 488-conjugated goat anti-chicken IgG
RARA	Rabbit	RPalpha(F)	Gaub et al., 1992*	Cy3-conjugated donkey anti-rabbit IgG
RARG	Rabbit	8965S	Cell signaling	Cy3-conjugated donkey anti-rabbit IgG
REC8	Rabbit	HPA031729	Sigma	Cy3-conjugated donkey anti-rabbit IgG
STRA8	Rabbit	ab49602	Abcam	Cy3-conjugated donkey anti-rabbit IgG
SYCP1	Rabbit	ab15090	Abcam	Cy3-conjugated donkey anti-rabbit IgG
SYCP3	Mouse	ab97672	Abcam	Alexa Fluor 488-conjugated donkey anti-mouse IgG

771 **Suppl. Table 1. Antibodies used in immunohistochemistry experiments.** *Gaub
772 *et al.*, (1992) *Exp. Cell Res.* 201:335-346.

Gene	Forward primer sequence (5' to 3')	Reverse primer sequence (5' to 3')	Amplicon size (bp)
Actb	CTAAGGCCAACCGTGAAAAGAT	CACAGCCTGGATGGCTACGT	195
Dazl	GTCCTTACATGTACCATTCTGTGAC	GACTCCAACAAAACAGCAGACAA	143
Ddx4	GTTGAAGTATCTGGACATGATGCAC	CGAGTTGGTGCTACAATAATACACT	299
Dmc1	GCGGCTACTCAGGTGGAAAG	TGGTCTACGTTGAAGCGGTC	97
Kit	CACTCACGGGCGGATCACAAA	CCACTTCACGGGCAGTCGTGC	106
Mei1	ACGCATCCAAAGCTGATGGAGGTT	CTTCAGCTCCAGGGTCAGTCGTAT	132
Meiob	GAACTGCATGGCAGCAACTG	GCTGTTCCACTGTATAGACATCA	188
Prdm9	TGGCTGATTACCAAGGGAAGAAAC	TCCCCATACCAGACCAGAAGCTCA	200
Rara	AAATCATCCGGCTACCACT	TCTGGATGCTTCGTCGGAA	73
Rarb	GTGTTCACCTTTGCCAACCAG	TTTAGTGCTTCCAGCAGTGGT	155
Rarg	TCTTCTGGCTACCACTATGGGGTCA	GCAGTACTGGCATCGATTTCTGG	147
Rec8	ATTCGACACCTTTTAGAGGCTG	AAGTCTCCTCGACTGATCTCTG	203
Smc1b	GCATGGATTGCTTGGAAGATA	CTGACGTTTTCCCTCATGGTT	158
Spo11	TTGATCCCACTGACAAAGCATGAC	GTCTGACGACAGCAAGGTCAAG	156
Stag3	GCTTGGAAAAGCACTTGGAG	GCTTCTGGCAAAGTCCACTC	155
Stra8	ACAACCTAAGGAAGGCAGTTTAC	GACCTCCTCTAAGCTGTTGGG	173
Syce1	GGAAAAGCATGGGGTACAGATCC	GCTGTCTCCTCGTGGACTTCTAC	105
Syce2	CAAGTCTGCCAAACTGTGGAAAC	GCAGAAGTCAGCATTCACCATCT	106
Sycp1	AGGACCGTTGGACAACGATTGC	CCTTGGTAAAGTTTGGCTCTCTTGG	160
Sycp2	GACACTGAAACCGAATGTGGA	TGTGGGTCTTGGTTGTCCTTT	165
Sycp3	GGGGCCGGACTGTATTTACT	AGGCTGATCAACCAAAGGTG	169
Tbp	TGCTGTTGGTGATTGTTGGT	AACTGGCTTGTGTGGGAAAG	99
Ugt8a	CTGCAGAGGTGGGTAAGTGG	GCAGGTCATTTTGAGGCAGCC	214

773 **Suppl. Table 2. Primers used for RT-qPCR on single cells.**